IMPERIAL COLLEGE LONDON

Department of Earth Science and Engineering

Centre for Petroleum Studies

Impact of Heterogeneity on Production in Tidal Sandstone Reservoirs: Application to the Linnorm Field, Offshore Norway.

By

Oluwole A. Talabi

A report submitted in partial fulfillment of the requirements for the MSc and/or the DIC.

September 2011

DECLARATION OF OWN WORK

I declare that this thesis *The Impact of heterogeneity on production in tidal sandstone reservoirs: Application to the Linnorm Field, offshore Norway* is entirely my own work and that where any material could be construed as the work of others, it is fully cited and referenced, and/ or with appropriate acknowledgement given.

Signature:

Name of Student: Oluwole A. Talabi

Names of Supervisors: Dr. Matthew Jackson and Prof. Howard Johnson

Acknowledgements

I gratefully acknowledge the help of all the people who have contributed in so many ways to make this thesis possible. I would like to express my gratitude to Dr. Matthew Jackson for providing me with the invaluable opportunity to work with himself and his team on this project. It has been a difficult, exciting and wonderful learning experience. I especially appreciate his insightful criticisms, patience, direction and guidance throughout the project. I owe my gratitude to Dr. Howard Johnson for providing support and guidance for the entire duration of the project. I would also like to thank Benoit Massart, whose excellent high resolution models served as a basis of all my work. I thank him for his continuous support and for his delightful enthusiasm throughout this period. To everyone who provided support and advice to me on this project: Dr. Jonathan Carter, Fahad Dilib, Oyekola Oyekole, Efe and many others too many to list here, I am truly grateful. I have learnt a lot from you all in a very short period.

I would also like to express my appreciation to the Petroleum Technology Development Fund (PTDF), Nigeria for sponsoring my MSc programme at Imperial College.

Finally, I acknowledge and remain forever grateful to my brothers Seyi and Segun, for their love, support, endurance and encouragement throughout what has been undoubtedly one of the most interesting and challenging years of my life.

Dedication

I dedicate this thesis to the memory of my late parents: Engr. Kolawole Talabi and Mrs. Olusola Talabi whose love made me all I am today. This one's for you.

Table of Contents

List of Figures

List of Tables

Imperial College
London

Impact of heterogeneity on Production in Tidal Sandstone Reservoirs: Application to the Linnorm Field, Offshore Norway

Oluwole A. Talabi

M. D. Jackson, H. D. Johnson, B. Y. G. Massart

ABSTRACT

Heterolithic tidal sandstone reservoirs feature in many recent discoveries and are of growing economic importance worldwide. However their properties are difficult to predict using conventional data due to the presence of heterogeneities characterized by complex inter-bedding of sandstone and mudstone.

This project focused on obtaining reservoir flow properties at a scale which is larger than is available from conventional core datasets. A generic 3m X 3m X 1m model of sandy tidal bar deposits, constrained by outcrop data from the Dir Abu Lifa Member in Egypt as an analogue to the low permeability Linnorm gas field, offshore Norway, was flow simulated over a range of fractional mud drape coverages to obtain effective properties. The mud drape coverage was linked to a more general petrophysical parameter- the volumetric net-to-gross (V_S) of the system. A set of direct relationships between effective permeability in the three principal directions and the net to gross (V_S) of the model were quantified. Over the range investigated, horizontal strike permeability reduces by 84% while horizontal dip permeability reduces by 68%. The vertical permeability declines at a faster rate than in the horizontal plane over the same range with a 99% reduction in vertical permeability. The vertical to horizontal permeability ratio reduces by a maximum of 96% over the same V_S range.

Horizontal anisotropy sets in at a V_S between 0.7 and 0.8 at this scale which suggests that production schemes with flow in the strike direction may be advantageous compared to flow in the dip direction but there is a variation in the orientation of the tidal bar units spatially therefore this may not be true at the field scale. No transition to effective 'non-reservoir' can be observed since the minimum volumetric V_S modeled (0.64) remains above documented percolation thresholds.
However, a transition to log-linear relationships between effective flow properties and V_S is observed in the same V_S range. These transitions are related to system-specific percolation thresholds which can be used to define property cut-off values. These cut-off values for horizontal and vertical permeability in Linnorm are estimated at 0.1mD and 0.02mD respectively.

1. INTRODUCTION

The economic importance of heterolithic tidal sandstone reservoirs in the world has been on the increase as they feature in many recent discoveries, most notably in offshore Norway as well as world-wide in places like Alaska, Canada, Venezuela and Russia (Martinius *et al.* 2005). These reservoirs are heterolithic sandstones, which are made up of complex intervals of inter-bedded sedimentary features ranging from thin lenticular sands in mudstone to mud flasers in sandstone (e.g. Martinius *et al.* 2005). The extent of these small-scale (millimeter to centimeter) intercalations vary greatly both laterally and vertically and indicate variation in the energy of the sedimentary depositional processes (Reineck and Wunderlich, 1968), characteristic of tidally-influenced depositional environments. During one tidal cycle, one flood and ebb current stages alternate with a slack-water period occurring after each of these two stages. During the slack-water periods, the tidal current is very weak so clay and silt are deposited from suspension and create more-or-less continuous mudstone layers called mud drapes (Nio and Yang, 2001). These mud drapes are more or less preserved by the erosive action of the tidal current.

The presence of these heterogeneities leads to complex sedimentary architecture, especially in 3D (Jackson *et al*, 2005), and consequently leads to a high degree of spatial irregularity in reservoir properties such as permeability, capillary pressure and mobile oil saturation, making them difficult to predict for use in engineering studies (e.g., Norris and Lewis, 1991; Martinius *et al.* 2001). In addition, the mud drapes can act as barriers to fluid flow (Ringrose *et al.* 2005) and affect reservoir performance. Previous experience in Norway has shown that improved reservoir description and modeling can lead to better field development and by extension, improved recovery which translates to significant economic benefits. (e.g. Martinius *et al.*

2005). Therefore reasonable modeling procedures should be followed in order to capture the effect of the important elements in the system (e.g. Kjonsvik *et al.* 1994; Jones *et al.* 1995). For tidal sandstones in particular, their complex inter-bedded nature makes it difficult to model them for flow simulation using conventional modeling techniques (Jackson *et al.* 2003).

Typically, in reservoir models, permeability variations are represented on a block-centered grid using values obtained from core-plugs, wireline-log data and well test analysis which are incorporated into the reservoir grid-blocks. There is a problem with this approach, especially in tidal sandstones because of the significant variation of properties with length scale. Core data are usually sampled at the mm~cm scale and do not capture the variability of facies whereas well test analysis samples at the 100m~km scale and averages over many different facies. None of these measurements are directly applicable at the typical reservoir simulation gridblock scale which is generally about 10's – 100's of metres. Thus upscaling permeability in a manner that yields representative effective values is difficult (Renard and de Marsily, 1997). Further, it has been shown that core-plug measurements of heterolithic sandstones are unlikely to be appropriate at the scale of a reservoir model grid block (Corbett & Jensen, 1991; Jackson *et al.* 2003).

Attempts have been made to bridge this gap by incorporation of two-dimensional (2-D) outcrop data (e.g. Oost and Baas, 1994), using three-dimensional (3-D) descriptions from larger outcrop rock specimens of varying size (Jackson *et al.* 2003; Jackson *et al.* 2005) and applying stochastic 3D models (Ringrose et al, 2003; Ringrose et al, 2005). These have improved understanding of the impact of heterogeneities in tidal sandstones and helped quantify the influence of parameters such as sandbody connectivity on oil recovery in these reservoirs (Jackson *et al.* 2003; Jackson *et al.* 2005, Brandsaeter *et al.* 2005).

Based on the results of these earlier works at varying scales, it has been shown that both individual and averaged effective permeability values vary as a function of sample volume and that permeability data from from core-plugs will not be representative at the scale of a reservoir model grid-block regardless of the number of measurements taken (Jackson *et al.* 2003.) It has also been shown that estimates of flow properties and connectivity based on 2D data are misleading when applied to 3D studies. Therefore an approach at a significantly larger scale, which is based on 3D data is warranted.

The aim of this project is to characterize the impact of one of such heterogeneities: Sandy tidal bar cross bed sets along which mudstonelayers (mud drapes) are deposited, on reservoir characterization and production. Effective permeability variation with mud content is obtained by flow simulation of a model based on data from a detailed 3-D description. This 3-D model is at a scale which is much larger than typical core plug data and possibly closer to a representative elementary volume (REV) as described by Bear (1972). The REV defines a specific volume-scale at which large variations due to heterogeneities are homogenized to provide a statistically representative single value (Norris and Lewis, 1991). For reservoirs with multiscale heterogeneities, this is the minimum sample volume from which data for upscaling should be obtained. It has been shown by Jackson *et al*. (2003) that a facies-REV can be achieved at around a 30cm length scale for tidal heterolithic layering.

Similar simulation studies have been used to quantify the effect of heterogeneities on flow with some success (e.g. Willis and White, 2000). For the work presented here, a generic 3m x 3m x 1m high resolution 3D-model of tidal bar deposits, constrained by outcrop data analogue, was constructed (Massart, 2011) using surface-based modeling techniques as described by Sech *et al*. (2009). This model captures the spatial distribution of the mud drapes in the sandy tidal bar cross-bed sets and also factors in their scale variability in terms of frequency, distance between them and their continuity in the model. The 3D-model is built using the Dir Abu Lifa member, Egypt as an analogue to the sandy tidal bar facies association in tide-influenced heterolithic sandstone deposits of the Ile and Tilje Formations in the Linnorm Field in Norway. The Linnorm field (previously Onyx) is a gas field owned by Norway's state-owned Petoro group; Total, Statoil and Norske-Shell.

There are two main objectives of this project. The first is to quantify the effect of the mud drapes on the effective permeability of heterolithic tidal sandstone systems dominated by sandy tidal bars and identify how they may be predicted using subsurface measurements. The second is to identify the transition between 'reservoir' and 'non-reservoir' – where the system becomes essentially uneconomic for gas production with specific application to Linnorm. This project has the potential to significantly improve the economics of Linnorm development by improving understanding of the fluid flow behaviors in such reservoirs.

2. LITERATURE REVIEW

2.1 Geological setting

The Linnorm field. The Linnorm field was discovered in 2005 and contains an estimated 60 billion cubic meters of gas. It is located in the Halten Terrace, and lies in a "growth area" under the PL 255 license where several other fields are in production or under development (Figure 1). The field spans the Jurassic Ile, Tofte and Tilje formations. All three formations correspond to tidally-influenced heterolithic sandstone reservoirs; with most of the hydrocarbon reserves in the Ile and Tilje formations. Trapping is due to faulting (gently tilted half-grabens) as is typical of reservoirs in the Halten terrace and these formations are mostly fluvio-deltaic sandstone units with varying degrees of tidal influence (Martinius *et al.* 2005).

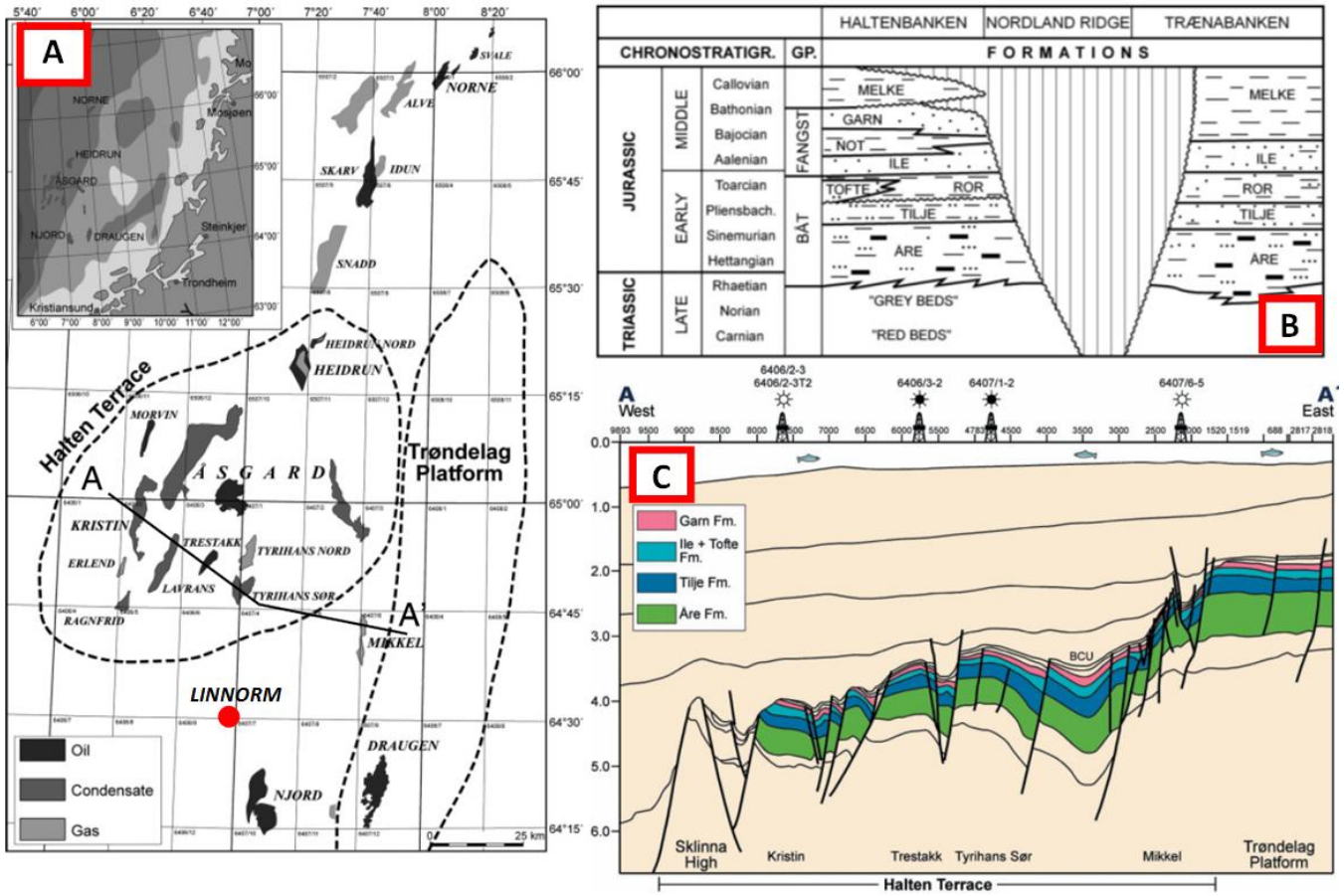

Figure 1: Linnorm field geology A) Map showing hydrocarbon fields in the Halten Terrace. The Linnorm field is indicated by the red dot. B) General lithostratigraphy of the mid-Norwegian continental shelf showing the Ile, Tofte and Tilje formations. C) Structural cross-section (A-A' on Fig. 1A) through the southern Halten Terrace showing the typical structural closures of reservoirs - fault planes dip westward (Martinius *et al.* 2005).

The average permeabilities encountered are very low (Table 1) particularly in comparison to other fields in the region because the field is in a more deeply buried zone. The mudstone permeabilities are below the resolution of the minipermeameter which explains the abnormal standard deviation and the very low geometric average.

Table 1. Minipermeameter measurements of permeability in cores taken from Linnorm

Measurement (mD)	Sandstone	Mudstone
Arithmetic Average (mD)	0.2423	0.0004
Geometric Average (mD)	0.116	< 0.0005
Standard deviation (mD)	0.0074	0.0012
Standard deviation (%)	3	300

Dir Abu Lifa Analogue. Data on Linnorm is limited (only core data are available) and so the model used in this project was built using the Dir Abu Lifa outcrop member of the Late Eocene deposits of the Fayoum Depression in the Western Desert, Egypt (figure 2), as an analogue for the Halten Terrace reservoirs in order to develop a better understanding of the depositional environment and facies distribution.

The Dir Abu Lifa Member is 77 m thick and comprises diverse lithologies. The unit can be divided into 8 sections (Bown & Kraus, 1988) of which only the bottom two (a thick cross bedded sandstone and a muddy sandstone) were used in developing the model.

Four main facies associations are seen in this giant cross-bedded sandstone of the lower Dir Abu Lifa Member (Legler *et al*, 2010): 1) channel-base mud, 2) inclined heterolithic strata tidal bars, 3) sandy tidal bars and 4) sigmoid heterolithic strata (SHS) tidal bars. The model used in this project was the Sandy tidal bar facies association is also illustrated in Figure 2.

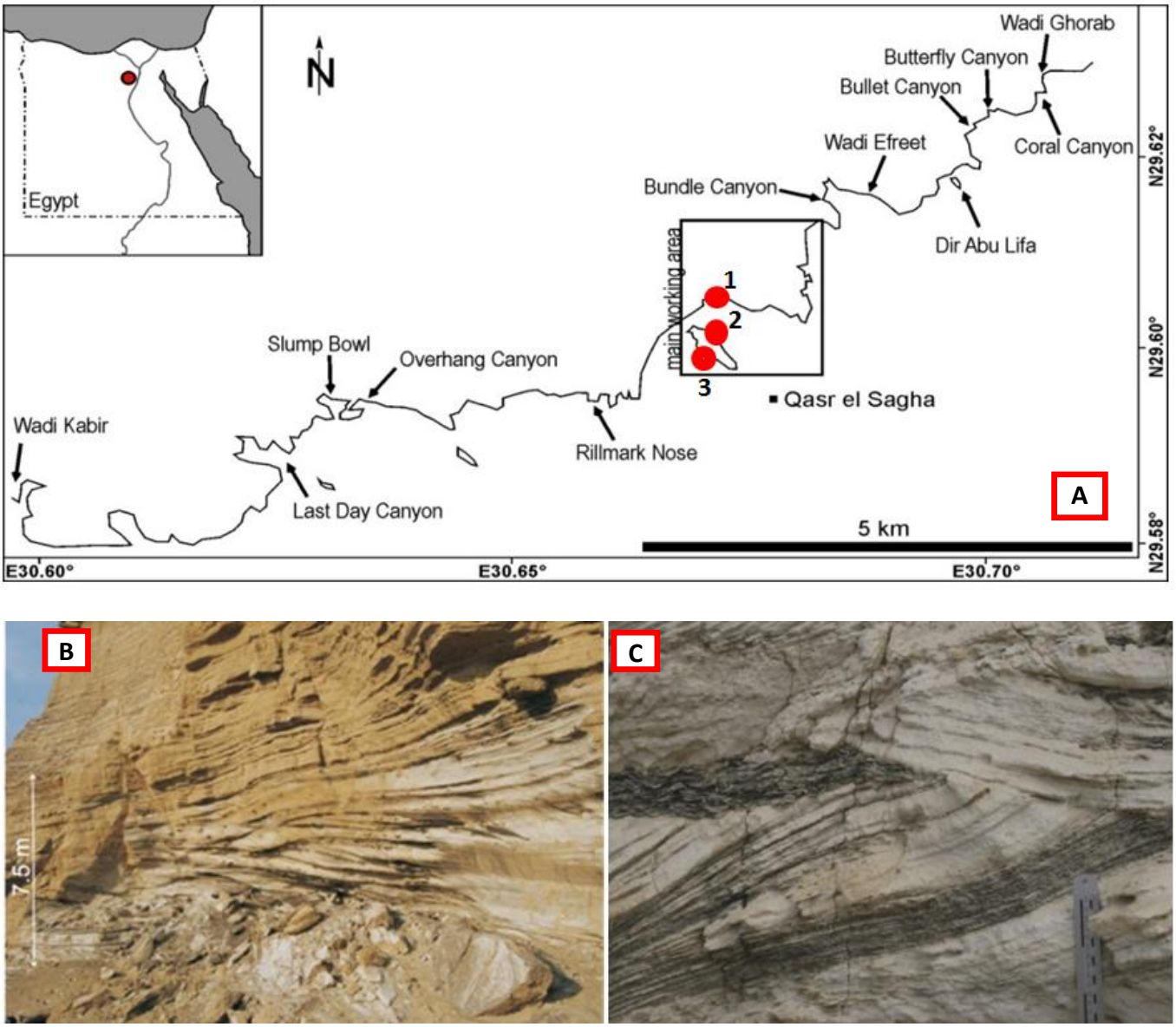

Figure 2: A) Location of the Dir Abu Lifa in the Fayoum depression (Bown & Kraus, 1988) and close-up of the study area (Legler *et al.* 2010). Locations of the outcrops chosen for analogue description and small-scale heterogeneity characterization are shown as red dots: 1- Gecko Nose; 2-DeadArm Wall; 3-Igel Wall. B) and C) Sandy Tidal bar facies association in the lower Dir Abu Lifa Member. It contains very fine- to fine-grained sandstone. Stacked sets of dune cross-bedding are visible with mud drapes and tidal bundles which are captured in our model. They are several meters thick and tens of meters in lateral extent.

2.2 Model Construction and gridding for simulation

The 3D model used in this work is a generic 3m x 3m x 1m high resolution section of sandy tidal bar deposits built using surface-based modeling techniques adapted for 3-D flow simulation (e.g. White and Barton, 1999; Jackson *et al.* 2005; Sech *et al.* 2009). Figure 3, illustrates the procedure adapted collecting this data. Details of the methodology used to construct the 3-D-models is detailed in Massart (2011) and summarized below:

1. The rock volume of interest was defined and subdivided into smaller volumes, defined by a top and a base surface, called ‘elemental volumes’ in which the heterogeneity surfaces have the same geometry.
2. A dataset was generated using photomontages and measurements of the outcrop parameters
3. 3-D template surfaces for each heterogeneity geometry were defined based on their geometry, and distributed according to outcrop observations (i.e. forest thickness, toeset thickness, foreset curvature and dip angle)

4. The mud drapes were inserted orthogonal to the dipping template surfaces as elliptical patches in 3D along the heterogeneity surfaces using a similar methodology to one used by Jackson & Muggeridge (2000).
5. The position and dimensions of the mudstone patches are chosen using probability functions of mudstone deposition.
6. The mudstone patches are added along the heterogeneity surface until the required proportion of mudstone (linked to mudstone distribution functions from outcrop analogue observations) is reached. This was done to create 17 cases with the proportion of mudstone coverage on each surface varying from 0 to 100%.
7. The model was built from the base elemental volume so sandy tidal bar units are created by stacking multiple dune cross-bed sets over each other.

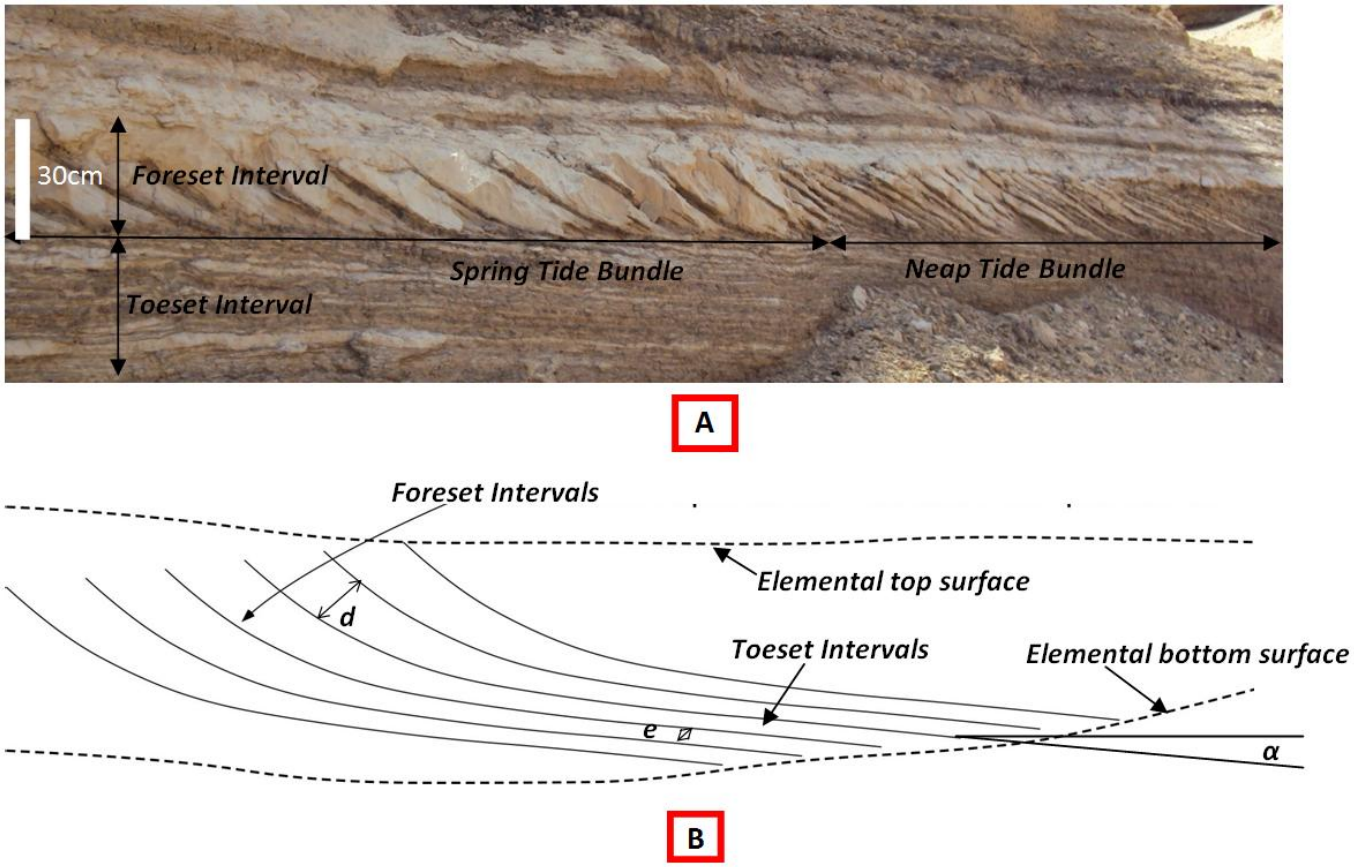

Figure 3: Illustration of building models from outcrop data. A) Spring and Neap tidal bundle in the Dir Abu Lifa member, Egypt. Sandy foresets/ muddy toesets and double mud drapes are visible along with the variation in thickness based on the depositional tide. B) Correlation and extraction of parameters to build surface model. Note the top and bottom elemental volume surfaces, labels: d – Foreset Thickness, e – Toeset thickness, α – Mean dip angle.

During model construction, the following rules were applied in order ensure the model was suitable for input into a flow simulation grid (White and Barton, 1999; Jackson *et al.* 2005):

1. All surfaces and zones are continuous across the model
2. Wherever a zone pinches out, it remains defined but is assigned zero thickness (the upper and lower bounding surfaces coincide)
3. None of the surfaces are allowed to cross each other
4. Surfaces must be vertically monotonic (no overhanging surfaces)

A 3-D corner point grid suitable for flow simulation was constructed from the model of sandy tidal bar deposits. Corner point gridding was used in order to capture the geological heterogeneity in detail. Corner point (distorted) grids, as introduced by Waldsley (1980) and Goldthorpe and Chow (1985) can adapt to reservoir boundaries, faults, surfaces, horizontal wells and flow patterns and are can be used in standard finite difference reservoir simulators. Corner point gridding helps usavoid using numerous, small-sized grid cells and consequently, increased computational time which would be needed if a conventional Cartesian grid were used. Simple Cartesian grids are quite common but their limitations in terms of their inability to describe faults, pinch outs and discontinuities accurately makes them unsuitable for capturing high resolution details. In this respect,

corner point grids are more appropriate (Ding and Lemonier, 1995). The methodology applied to construct the corner point grid used here is similar to the one used by White & Barton (1999) which was developed and applied for 3D-modelling of heterolithic tidal deposit models by Jackson *et al.* (2005).

The grid constructed is regular, having 100 grid blocks in *i* and *j* dimensions with each cell measuring 3 cm. In the *k* dimension, the grid is irregular due to the numerous dipping surfaces and pinchouts. All the cells between any two surfaces (i.e. within a zone) have a constant thickness of 2 cm. The number of blocks in the z direction is always the same, which keeps the number of blocks in each zone between two surfaces of the grid fixed, despite the numerous pinch outs. Although the resulting grid is defined by 9.8 million cells it does not require upscaling for flow simulation because of the nature of the corner point gridding scheme used to represent the complex facies architecture. It is constructed according to the rules given above and so the grid structure is controlled by the surfaces. This leads to an efficient gridding scheme where only about 6% (589682 for the X and Y permeability and 609682 for the Z permeability cases) of the grid blocks in the simulation are active in any given run. The grid blocks along the mud drape surfaces are designated as mud stones and so the thickness of the mud drape surfaces are controlled by the grid block thickness which is 2 cm. The modeled mud drape thickness is thus controlled by the minimum grid block thickness. Toeset thickness observed at outcrop ranged from 2 mm to 5 cm with an average of 5mm, however since each toeset layer is composed of one sandstone and mudstone layer with a vertical to horizontal permeability tending towards zero, the exact thickness of the mudstone does not have significant impact on the results.

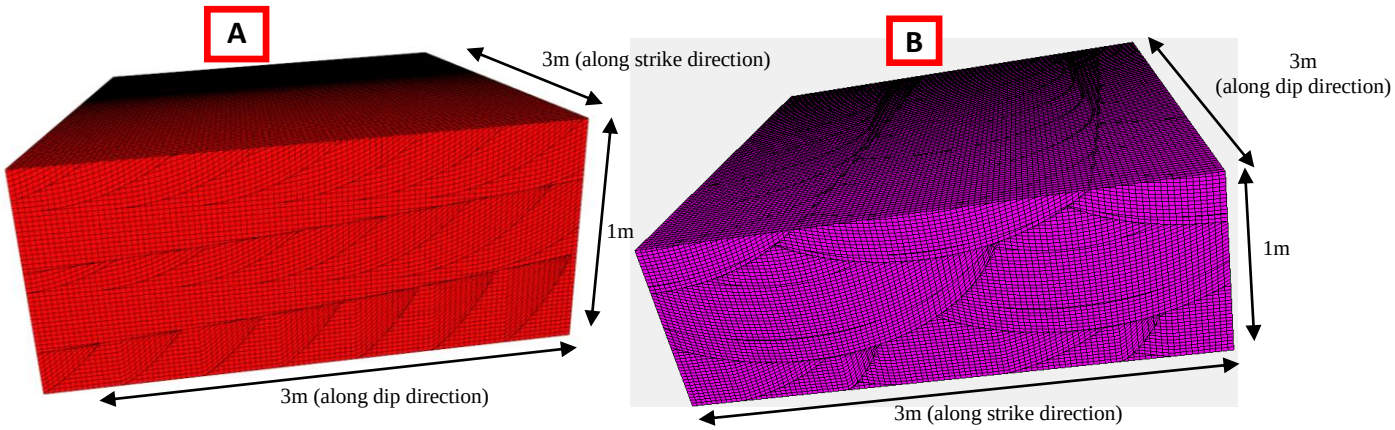

Figure 4. 3-D grid used for flow simulation. The dimensions are indicated. The frontal face shown in A) is the end face of the model as seen from a cross-section along the depositional dip direction and B) indicates the depositional strike cross section.

Although corner point grids are more efficient than Cartesian grids for flow simulation, the grid introduces artifacts in the in the solution to fluid flow equations. The lack of orthogonality in the system implies that the permeability tensor is not diagonal. However, most commercial simulators assume the equations have diagonal permeability tensors and that flow occurs across faces that are perpendicular to them. For highly non-orthogonal grids, this is not the case and corner point grids can introduce large errors in flow simulations (Wu and Parashkevov, 2005). These limitations, especially the effect of non-orthogonality on the accuracy of simulation results, have been documented in the literature (e.g. Ding and Lemonier, 1995; Peaceman, 1996) but as yet there appears to be no standard method for estimating the size of the error introduced by non-orthogonality (Bagheri and Settari, 2003). These errors, their impact on the results obtained from this work and possible means of mitigating them based on concepts established by Aavatsmark et al, (1996) are discussed in section 4.

3. FLOW SIMULATION METHODOLOGY

Permeability is defined in the principal axes of the permeability tensor referenced to the outcrop (X – along the dip direction, Y – along the strike direction and Z – vertical) and the simulations were designed and run to generate effective permeability in these directions. The simulations were designed to mimic the setup of conventional core experiments to measure permeability. The simulations were performed using Schlumbergers ECLIPSE© 100 software.

17 models were constructed with the proportion of probabilistic mud drape coverage along each surface ranging from 0 to 100%. The lower extreme represents a case in which mud drapes are not present at all and corresponds to a model fully populated by sandstone in which only the reservoir structure (grid) has any effect on the simulation while the lower percentages represent cases of fully developed mud drape coverage along the entire surface. Tests were run with all cases in each direction to adequately capture the change of permeability across the range.

For this study, focus is placed on the mud drape surfaces as flow controls because the sharp contrast in properties between the sandstone and the mudstones is deemed to have the most significant impact. It also more clearly focuses the simulation on the effects of the reservoir heterogenieties than on property interactions or other factors. This is similar to the approach used by Jackson *et al.* (2009) to study geologic flow controls in a shoreface-shelf parasequence.

3.1 Model structure

The model dimensions are 3m X 3m X 1m and the number of grid blocks is 100 x 100 x 988. Due to the nature of the gridding as explained in section 2.6, only about 6% of the total number of defined grid cells are active in any given run. For effective permeability in the X and Y directions, the two cells in the layers at the end of each direction are assigned very high permeability so that they act as a 'buffer' in order to permit approximately instantaneous flow into this layer and allow uniformly distributed flow focused in the direction of interest. This buffer permeability is 54 x 10^6 mD; a value obtained by approximating them to be open fractures of width ~3cm based on combination of viscous force equations and Darcy's law. This methodology ensures cells in the buffer layer are equipotential in any given time step. These buffer cells mimic the effect of meshes used to distribute fluids evenly in a core during routine core analysis (Figure 5).

A similar approach was used with simulation in the Z direction but in this case, since the vertical layers are irregular, two extra layers of uniform thickness were added at the top and bottom. These were used as the buffer layers for these runs, making the dimensions of the grid used for these simulations slightly larger (3m x 3m x 1.04m – 100 x 100 x 990)

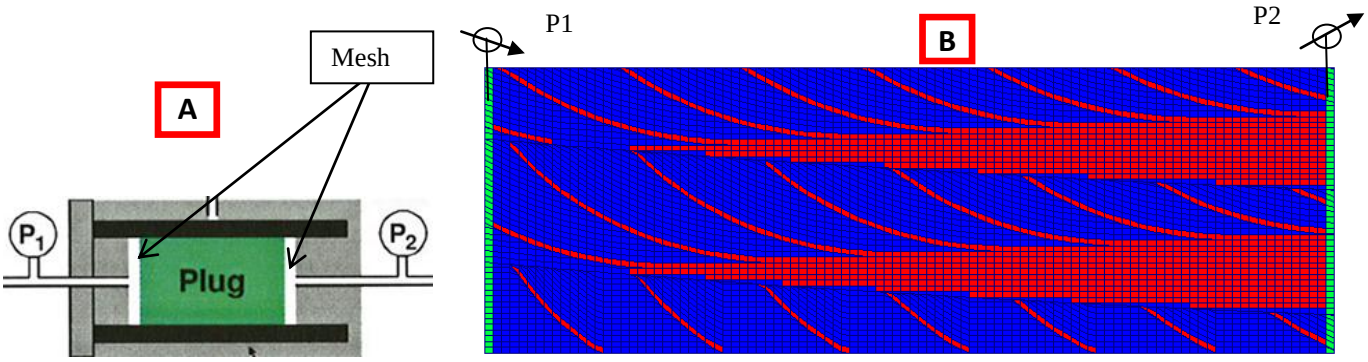

Figure 5: Illustration of simulation strategy showing analogy with typical core flood experiment. A). Schematic diagram of typical core flood experiment. P1 and P2 are the injection and production pressures respectively, mesh is also indicated B). Section along X-axis of the steady state model showing similarity to core experiment. Cells in green correspond to permeability of open fracture (54 x10^6 mD) to mimic mesh used in the core cell. Blue corresponds to sandstone cells and red indicates impermeable mudstone cells

3.2 Rock and fluid properties

The models were populated with two sets of permeability for each facies: sandstone and mudstone. All sandstone cells were assigned the same uniform isotropic permeability value. The mudstone facies were assigned zero permeability in the grid blocks along the mud drape surfaces where they occur hence the mud drapes are modeled as thin, single-layer zones of mud (2cm thick) which are completely impermeable.

Incompressible water with a viscosity of 0.31cP and formation volume factor of 1.0 cc/std cc was used for estimating the effective permeability of the model. Capillary pressure is neglected.

3.3 Simulation strategy

The strategy used here is similar to that used by Warren and Price (1961). The model was saturated with water and simulated by injecting water into each grid block at the inlet layer and producing from each grid block at the outlet layer until steady state is reached. Steady state in this case was deemed to have been reached when constant, equal flow rates from faces as well as constant average model pressure were obtained. These rate and pressure data, as well as the tolerances are presented in section 4). The results were used to calculate effective permeability values as described in section 3.4. Preliminary checks indicated that the calculated permeability is independent of the input rate therefore simulations were controlled with rates chosen to procide ease of simulation for the specific case. No other limits were imposed.

A similar methodology was used to observe the fluid flow path by injecting tracer with the injection fluid along the strike direction. Flow was simulated in the models between opposing faces and assuming no flow across the other faces in much the same manner that the effective permeability was calculated.

Tracer-saturated water (tracer concentration of 1) was injected into water saturated model. In the simulations, tracer diffusion was kept at zero so only convective flow with water under the imposed pressure gradient is produced. Since mudstones are assigned zero permeability, flow only occurs only through the sandstone layers. These tracer simulations are therefore a reasonable method of observing the flow path taken by injected fluid during a multiphase displacement and the method is similar to that used by Jackson *et al.* (2005) to quantify displacement efficiency in heterolithic tidal sandstones.

3.4 Effective permeability calculations

The results from these simulation experiments are used with the appropriate simplifications to calculate the effective permeability (k_{eff}) across the model. Darcy's law is used for these calculations with the same assumptions and boundary conditions that were used in the simulations i.e. incompressible fluid, no capillary pressure, single phase and one-directional flow. The equation simplifies to:

$$k_{eff} = \frac{q_w\ \mu_w \Delta L}{\Delta\theta_c A} \quad \text{.......................................} \quad (1)$$

The corrected potential (θ_c) is the average pressure in each buffer layer, corrected to the same depth to remove the effect of gravity on the cell pressures. A is the cross-sectional area across which the fluid flows. The effective permeability (k_{eff}) for each case is normalized to the base case (the 0% mud drape coverage) permeability for that direction (k_{eff-0}) so that the impact of the increased mud drape coverage can be quantified without being dependent on the actual value of permeability used in the simulations and thus, more generally applicable. It also desensitizes the model to errors introduced by the corner point grid. The k_{eff} values were calculated as a ratio of the effective permeability for that case to the permeability of the fully homogenous case in that direction. These ratios for each of the *x*, *y* (horizontal), and *z* (vertical) directions, are expressed in terms of a *dimensionless* permeability k_n for that direction. Subscript *i* in equation 1 refer to the direction of flow. Examples of the simulation files and the results of effective permeability calculations are presented in the appendix

$$k_n = \frac{k_{eff}}{k_{eff-0}} \quad \text{.......................................} \quad (2)$$

Test grids and preliminary checks.

The methodology was verified by simulating flow through a completely homogenous and isotropic model measuring 100 x 100 x 50 with the same dimensions as the high resolution model. The results from this grid were compared with tracer and effective permeability results from the high resolution grid. These testcases reproduced their input permeability, thus validating the method. In addition, a test using the high resolution grid populated with homogenous permeability was used to check for any possible grid effects on the results. The tests indicate that the results are approximately 10% different from the input homogenous permeability. This kind of error is not unexpected with highly non-orthogonal grids as explained in section 2.5 and the effects of the error and its impact on the results are discussed in section 4.

3.5 Correlation with Volumetric Sandstone fraction.

The volumetric sandstone fraction (V_S) for each case was calculated and correlated with the corresponding percentage mud drape surface coverage in order to apply the results to reservoir characterizarion. The sandstone connectivity and V_S for heterolithic sandstones is highly variable and depending on the sample (flaser, lenticular or wavy bedding), different V_S values may be obtained for the same formation (Jackson *et al*, 2005). This may be observed visually in our model where there is higher V_S at the foreset area than the toeset area. This is consistent with the outcrop observations.

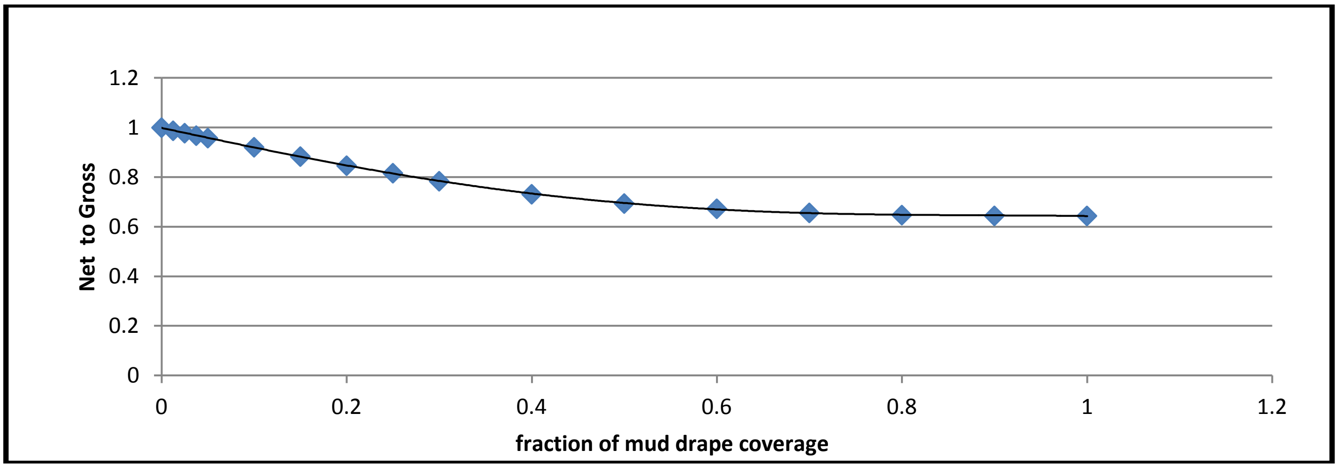

Figure 6. V_S variations with fractional mud drape coverage.

The V_S obtained here was fit to a quadratic function (figure 6 and equation 3) of fractional mud drape coverage which was used to interpolate for mud coverage (m) and corresponding effective permeability values. The goodness of fit (R^2) for this correlation is 0.9991.

$$V_s = 0.5073m^2 - 0.8535m + 0.9985 \quad \ldots \ldots (3)$$

The V_S in the model used for the study varies between of 1 with no mud present and 0.644 at maximum mud drape coverage.

4. RESULTS

Tables 2, 3 and 4 present the input data and results used to calculate the effective permeabilities from the simulation experiments for the X, Y and Z directions. The resulting normalized permeability data is presented in figure 7. Figure 7A shows the variation of the normalized effective permeability as a function of the V_S for flow in the *x y* and *z* direction as well as the variation of the average normalized vertical to horizontal permeability ratio with V_S. As expected, all the permeability values reduce with reduced V_S. The normalized effective permeability in the *x* (k_{nx}) and y (k_{ny}) directions are initially approximately the same but begin to diverge at a V_S of about 0.8 with k_{ny} eventually becoming double the value of k_{nx} at the minimum V_S of 0.644 making the system effectively anisotropic. The at the maximum mud drape coverage (minimum V_S) k_{nx} drops down to 16% of its initial value which indicates an 84% reduction in permeability over the range. A similar drop is seen with k_{ny} but this value only reduces to 32% of the original. The normalized effective vertical permeability (k_{nz}) decreases much more dramatically than k_{nx} or k_{ny} with decrease in V_S as the mud drapes become more laterally extensive. As can be seen in the figure, for k_{nz}, the reduction in vertical permeability between the V_S of 1 and 0.644 is approximately 99%. This heterogeneity-induced isotropy could possibly have significant implications for the development of such reservoirs. The same normalized permeability calculation results are presented on a semi-log plot in Figure 7B. An average normalized horizontal permeability (k_{nh}) was obtained by taking the average of the k_{nx} and k_{ny} for each model and the ratio between this k_{nh} and the normalized vertical permeability (k_{nz}) is computed and also presented as a function of V_S in figure 5. Due to the greater impact of the increasing mud coverage on the k_{nz} than k_{nh}, the normalized effective k_{nz}/k_{nh} ratio is dominated by the k_{nz} and follows a similar trend eventually reducing to 4% of its initial value.

Table 2. Simulation input data and calculation results for X-direction

Mud drape coverage	Input Flow rate	Length of flowpath	Cross-sectional Area of flow	Potential difference	Input Viscosity	Effective permeability k_{effi}	Normalized Effective permeability
%	Q	L	A	ΔP	μ	mD	
0.00	5000	297	30000	0.06265	0.31	68.0384	1.0000
1.25	5000	297	30000	0.06382	0.31	66.7886	0.9816
2.50	5000	297	30000	0.06476	0.31	65.8170	0.9674
3.75	5000	297	30000	0.06573	0.31	64.8510	0.9532
5.00	5000	297	30000	0.06673	0.31	63.8776	0.9388
10.00	5000	297	30000	0.07093	0.31	60.0958	0.8833
15.00	5000	297	30000	0.07665	0.31	55.6121	0.8174
20.00	5000	297	30000	0.08364	0.31	50.9618	0.7490
25.00	50	297	30000	0.00092	0.31	46.2461	0.6797
30.00	50	297	30000	0.00104	0.31	41.0053	0.6027
40.00	50	297	30000	0.00136	0.31	31.3189	0.4603
50.00	50	297	30000	0.00185	0.31	23.0630	0.3390
60.00	50	297	30000	0.00236	0.31	18.0752	0.2657
70.00	50	297	30000	0.00305	0.31	13.9974	0.2057
80.00	50	297	30000	0.00356	0.31	11.9599	0.1758
90.00	50	297	30000	0.00377	0.31	11.3064	0.1662
100.00	50	297	30000	0.00377	0.31	11.2977	0.1660

Table 3. Simulation input data and calculation results for Y-direction

Mud drape coverage	Input Flow rate	Length of flowpath	Cross-sectional Area of flow	Potential difference	Input Viscosity	Effective permeability keffi	Normalized Effective permeability
%	Q	L	A	ΔP	μ	mD	
0.00	5000	297	30000	0.06050	0.31	70.45792	1
1.25	5000	297	30000	0.06173	0.31	69.05507	0.980089
2.50	5000	297	30000	0.06264	0.31	68.04573	0.965764
3.75	5000	297	30000	0.06370	0.31	66.91649	0.949737
5.00	5000	297	30000	0.06488	0.31	65.69457	0.932394
10.00	5000	297	30000	0.06924	0.31	61.56462	0.873778
15.00	5000	297	30000	0.07430	0.31	57.36993	0.814244
20.00	5000	297	30000	0.08028	0.31	53.09813	0.753615
25.00	5000	297	30000	0.08588	0.31	49.63587	0.704475
30.00	50	297	30000	0.00092	0.31	46.15593	0.655085
40.00	5000	297	30000	0.10464	0.31	40.73568	0.578156
50.00	5000	297	30000	0.11774	0.31	36.20160	0.513805
60.00	5000	297	30000	0.13748	0.31	31.00462	0.440045
70.00	5000	297	30000	0.15840	0.31	26.91044	0.381936
80.00	5000	297	30000	0.17941	0.31	23.75879	0.337205
90.00	5000	297	30000	0.18573	0.31	22.95049	0.325733
100.00	5000	297	30000	0.18662	0.31	22.84080	0.324176

Table 4. Simulation input data and calculation results for Z-direction

Mud drape coverage	Input Flow rate	Length of flowpath	Cross-sectional Area of flow	Potential difference	Input Viscosity	Effective permeability keffi	Normalized Effective permeability
%	Q	L	A	ΔP	μ	mD	
0.00	6000	100	90000	0.00680000	0.31	84.4227	1
1.25	6000	100	90000	0.00780000	0.31	73.5992	0.871795
2.50	1	100	90000	0.00000140	0.31	68.3422	0.809524
3.75	1	100	90000	0.00000140	0.31	68.3422	0.809524
5.00	1	100	90000	0.00000152	0.31	62.9467	0.745614
10.00	1	100	90000	0.00000210	0.31	45.5614	0.539683
15.00	1	100	90000	0.00000290	0.31	32.9928	0.390805
20.00	1	100	90000	0.00000420	0.31	22.7807	0.269841
25.00	1	100	90000	0.00000550	0.31	17.3962	0.206061
30.00	1	100	90000	0.00000810	0.31	11.8122	0.139918
40.00	1	100	90000	0.00001370	0.31	6.9839	0.082725
50.00	1	100	90000	0.00002890	0.31	3.3107	0.039216
60.00	1	100	90000	0.00006990	0.31	1.3688	0.016214
70.00	1	100	90000	0.00009340	0.31	1.0244	0.012134
80.00	1	100	90000	0.00010860	0.31	0.8810	0.010436
90.00	1	100	90000	0.00011050	0.31	0.8659	0.010256
100.00	1	100	90000	0.00011060	0.31	0.8651	0.010247

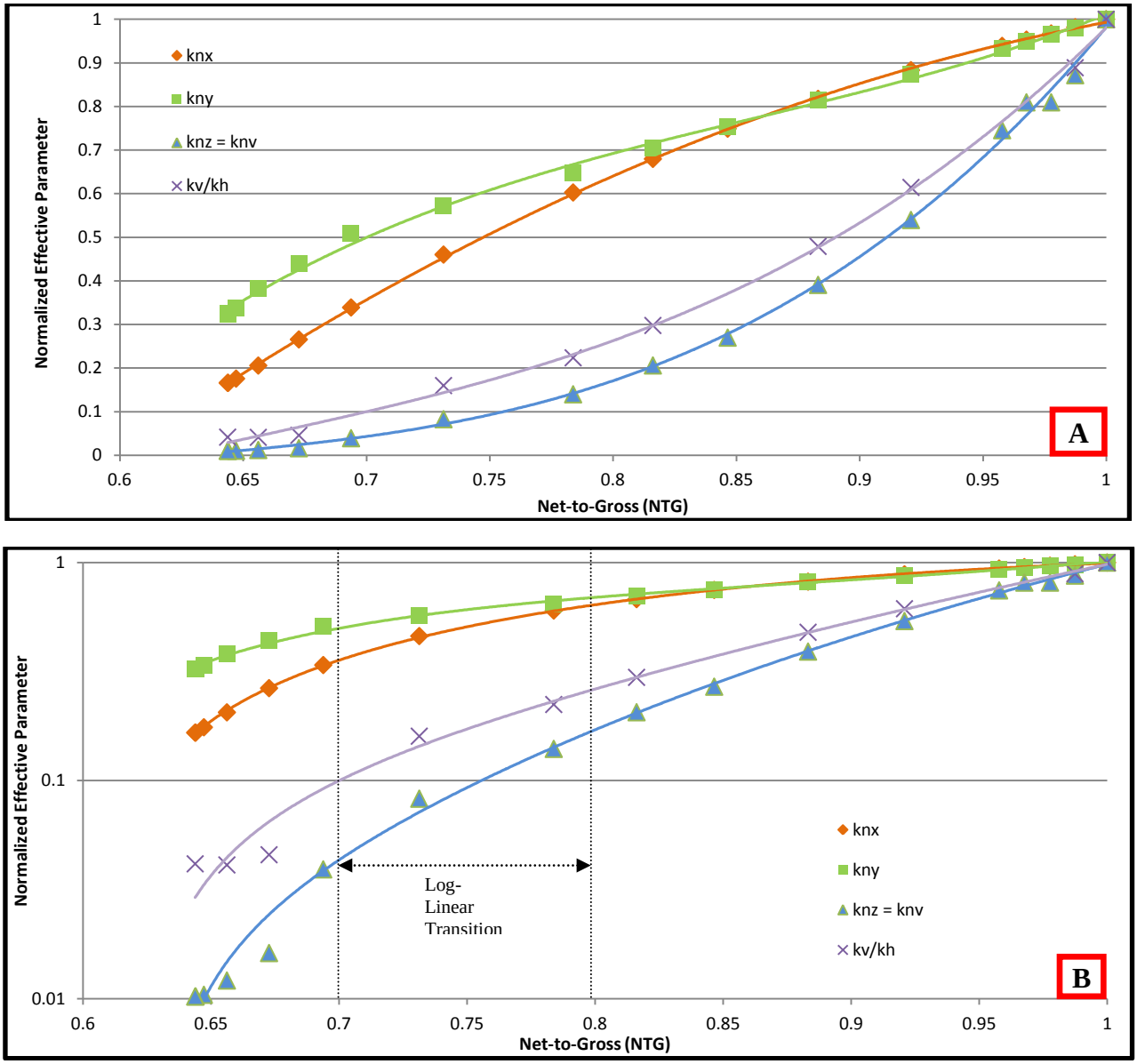

Figure 7. Effective permeability simulation results. Variation of k_{nx}, k_{ny}, k_{nz} and k_{nz}/k_{nh} with V_S and given in A). B) presents the same results on a semi-log scale and the transition region where the relationships become log-linear is indicated.

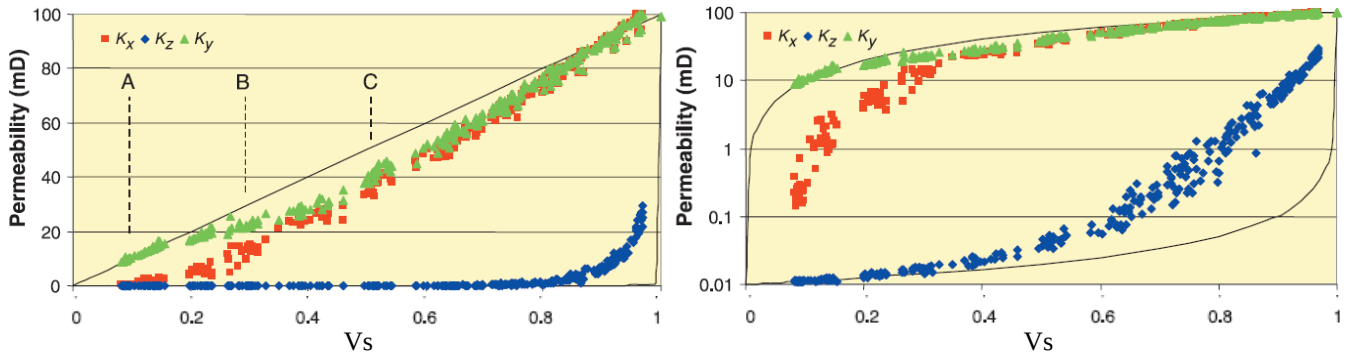

Figure 8: Effective permeability results of flow simulations from models of heterolithic bedding by Ringrose et al. (2005). Fig A) presents their effective permeability variation with mudstonevolume fraction in the model. The same results are presented on a semi-log scale in Fig B) and the transition regions related to percolation thresholds are indicated by points A, B and C.

These results are very similar to the high sandstone volume region of the results obtained by Ringrose *et al.* (2005) when they investigated methods for estimating vertical permeability in tidal sandstones using a 0.5 X 0.5 X 0.1m size model. Implications of these similarities are discussed in section 5. All normalized effective permeability results as well as the ratio of normalized effective vertical to horizontal permeability are correlated to V_S using simple polynomial equations (up to cubic) all within goodness of fit of at least 0.99.

$$k_{nx} = -3.5837(V_s)^2 + 8.2141(V_s) - 3.6372 \quad \ldots\ldots\ldots\ldots\ldots\ldots\ldots\ldots\ldots (4)$$

$$k_{ny} = 15.201(V_s)^3 - 39.108(V_s)^2 + 34.901(V_s) - 9.9815 \quad \ldots\ldots\ldots\ldots\ldots\ldots (5)$$

$$k_{nz} = k_{nv} = 14.288(V_s)^3 - 26.454(V_s)^2 + 16.813(V_s) - 3.6638 \quad \ldots\ldots\ldots\ldots\ldots (6)$$

$$\frac{k_{nv}}{k_{nh}} = 11.731(V_s)^3 - 22.791(V_s)^2 + 15.991(V_s) - 3.9499 \quad \ldots\ldots\ldots\ldots\ldots\ldots (7)$$

The results of tracer injection to show the flow path taken by fluids injected are observed visually in 3-D and cross-sections through the model are presented for flow along the strike direction (Figure 9). A comparison with flow through an orthogonal grid of similar dimensions at same conditions is also shown. There are grid artefacts in the results, especially where pinchouts occur and the grid faces are non-orthogonal to flow (indicated by point 1 and 2 on column ii of Figure 9). The grid artefacts however do not preclude the utility of these simulations in observing the impact of the heterogeneity surfaces on fluid flow. We can observe an obvious bias of flow to the toeset region of the model as the tracer advances faster in through that section. These tracer injection results establish a methodology for the observation of the flowpaths and although estimates of sweep effieciency were not calculated for this work, the methodology can be applied in a manner similar to that used by Jackson et al. (2005). This is the subject of continuing work on this project.

Accuracy and uncertainty. The potential values obtained from the simulation at steady state are consistent to 3 decimal places between timesteps and consequently, the normalized effective permeability values can only be reliably quoted to this accuracy.

However, the error associated with the non orthogonality of the grid is the most significant here and are summarised in table 2. The calculated permeability values are on average about 10% different from the expected value produced by a corresponding orthogonal grid of similar dimensions using isotropic permeability. The error is dependent on flow direction; horizontal permeability is under predicted in both x and y directions while vertical permeability is over predicted when using the non-orthogonal model. Based on inital tests (see Appendix), it appears that the magnitude of the error in each direction remains approximately the same regardless of specified flow rate. Further work to quantify the error may be warranted.

The directionality of the error is typical of the problems commonly encountered with corner point geometry as used here especially considering the dipping stratigraphy and pinchouts. For most commercial simulators, once the grid block face is not orthogonal flow direction across it and connections to other blocks, an error results: a variant of the well known "grid orientation effect" first demonstrated for five point block-centred reservoir simulators by Todd *et al.* (1972). Many researchers have proposed methods for reducing this error but for such highly non-orthogonal grids, only a consideration of all the components of the potential at block faces will overcome the error (Aziz, 1993).

Such a consideration of potential at all grid faces may be achieved using the multipoint flux approximation (MPFA) using more than two cells to calculate flow as introduced by Aavatsmark *et al*, (1996). The MPFA methods work by splitting a simulation grid into interaction regions and performing flux calculations for the interface between any two cells in the grid. The parameters used for the calculations are split between these interaction regions. For gridding systems composed of 3-dimesional quadrilaterals such as the one used in this study, an interaction region will generally contain contributions from eight grid cells. The part of a grid cell interface that lies within the interaction region is called a flux interface.

Table 2. Measurements of error associated with the simulations.

	Value(mD)	**Error (mD)**	**% Error**
Input Isotropic Permeability	77	-	-
Harmonic Average Permeability (accounting for buffer zones)	77.803	-	-
Permeability from Test grid (X, Y and Z)	77.785 ± 0.02	0	
X-Permeability from homogeneous corner point grid model	68.038	9.747	12.530
Y-Permeability from homogeneous corner point grid model	70.457	7.328	9.420
Z-Permeability from homogeneous corner point grid model	84.422	6.637	8.532
Average Error			***10.161***

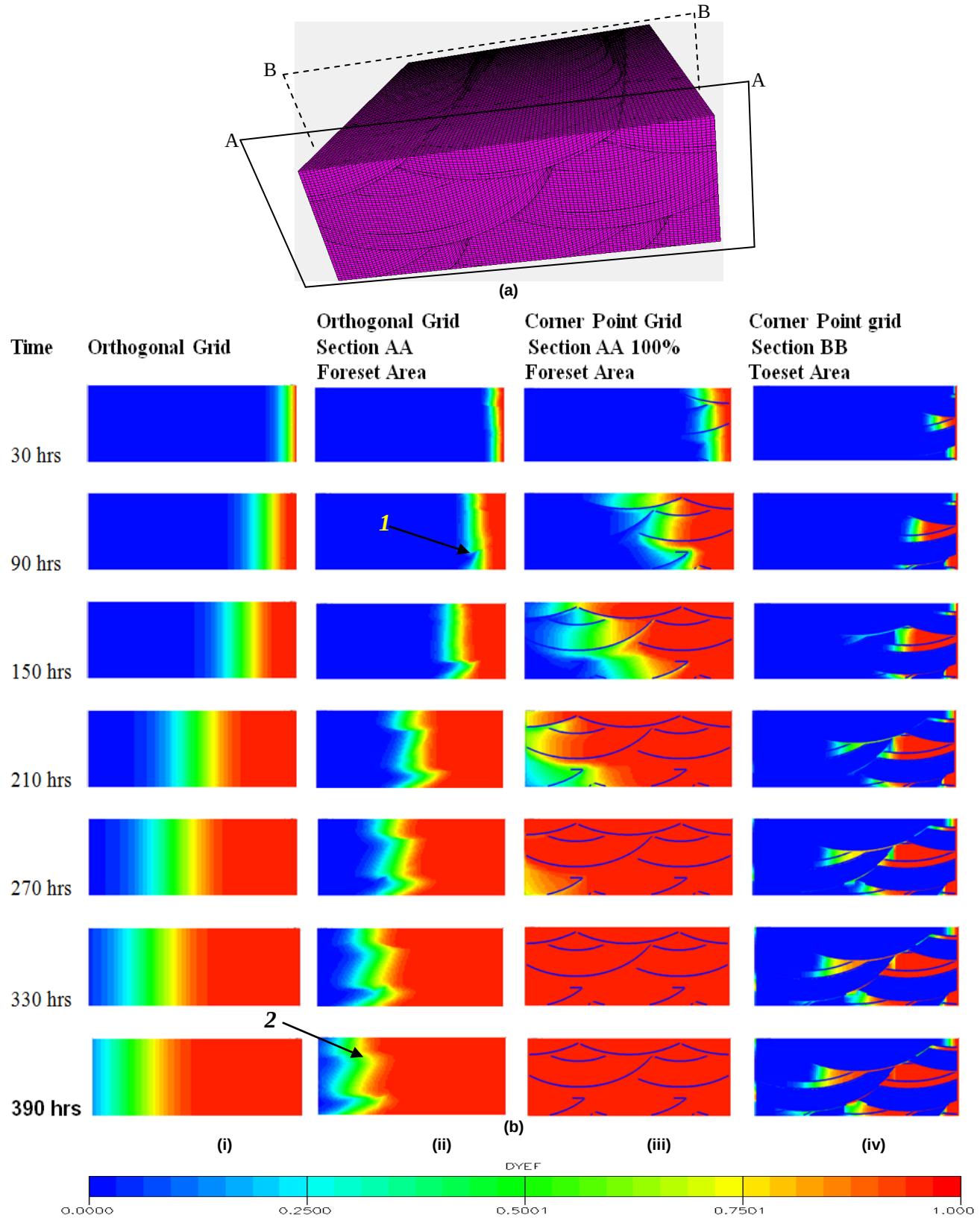

Figure 9. Time slices through models showing the fronts developed by injected tracer. Color scale indicates tracer concentration .Fig 9a shows the sections through which the slices are taken. Section AA goes through the foreset area and BB through the toeset area. Column (i) shows results through a test grid which is fully homogenous and orthogonal and the front is linear as expected. Column (ii) shows the same results for a homogenous case in our non-orthogonal model and the presence of grid artifacts are indicated. Columns (iii) and (iv) show the slices through Section AA (foreset area) and Section BB (toeset area) for flow through the high resolution model with maximum mud drape coverage. The influence of the mud amalgamations on flow path can be seen as flow is channeled primarily in the foreset area where mud drapes are not amalgamated. Flow through the toeset area is more restricted as the mud drapes amalgamate to form impermeable blocks.

A multipoint flux approximation may be obtained by taking the weighted sum of the potential values in grid cells within the interaction region (Aavatsmark *et al*, 1996). A wide range of MPFA methods exist and the 'O' and 'U' methods are the most common and stable. Only minor differences have been reported between the results from both methods. Their properties, derivation and formulations are discussed in detail by Aavatsmark *et al.* (1996) and use of these methods for flow simulation is currently being investigated as a means of reducing or eliminating these errors.

5. DISCUSSION

No evidence exists of economic production of hydrocarbons from formations with a matrix permeability of less than 10^{-6} D even after fracturing treatments (Bennion *et al*, 1996). Based on this evidence, we may classify the transition between economically 'productive reservoir' and 'non-productive reservoir' as being the point where the effective permeability is less than this value in any direction. We approximate sandstone permeability in Linnorm to be about 0.2mD (section 2.1), and define 'non- reservoir' to occur where the effective permeability of the field falls below 10^{-3}mD in any direction. No such transition can be seen to occur here and it is believed that this is due to the approach taken to model the mud stones i.e. the minimum volumetric V_S at the maximum mud converge is 0.64: well above the percolation threshold of King (1990).

King (1990) applied percolation theory to investigate the sandstone connectivity using a conceptual infinite system made up of square-shaped isotropic sand bodies. King (1990) observed a specific threshold value called the "percolation threshold" of the sandstone fraction below which there is no connectivity and thus correspondingly, effectively zero permeability. According to King (1990) this "percolation threshold" occurs when the sandstone fraction is 0.28 for a three dimensional system. The existence of this threshold value is proposed to be the result of sandbody isolation. At very low sandstone fractions, sand bodies are isolated from each other and so flow cannot occur through them over the entire system. However, with increased sandstone fraction, they overlap, forming connected groups which, at the threshold fraction, eventually occupy enough of the system to establish connectivity across it. Sandstone connectivity is likely to be the dominant control on the transition between reservoir) and no reservoir rock (King, 1990; King *et al.* 2001).

Ringrose *et al.* (2003) investigated percolation thresholds for heterolithic tidal sandstones and suggested that the percolation threshold differs for horizontal and vertical connectivity. They obtained values of 0.28 for the horizontal threshold (the same value predicted by King (1990)) and 0.5 for the vertical threshold (the difference is attributed to anisotropy). In any case, the model used here remains well above these reported thresholds and sandstone connectivity is maintained for the range investigated, hence the absence of a clear transition from 'reservoir' to 'non-reservoir' using the criteria cited earlier.

However, according to Ringrose *et al.* (2005), observation of the points at which the $k_{ni} - V_S$ relationships become log-linear are also related to percolation thresholds. This implies that the percolation threshold for the heterolithic tidal sandstone systems dominated by sandy tidal bar cross-bedding are different from those reported by King (1990) and Ringrose *et al.*, (2003) for generalized sandstone-mudstone intercalations. These thresholds are apparently unique to the system investigated and may be used to define petrophysical property cut-off values and obtain a net to gross estimate. It is also worthy of note that the onset of anisotropy in the horizontal plane begins at the same range of V_S. Results from this work indicate that this transition occurs between V_S of 0.7 and 0.8. Using a Linnorm permeability value of 0.2 mD and assuming a cut-off at the lower end of the transition (0.7), we can read off the corresponding normalized effective permeability cutoff values from figure 7 which gives a horizontal permeability cut-off value of about 0.1mD and a vertical permeability cut-off 0.02mD.

As noted earlier, these results bear marked some similarities to those obtained by Ringrose *et al.* (2005). Ringrose *et al.* (2005) used flow simulation of a 3-D volumes built to mimic deposition processes by the migration of bedding planes using vectors to investigate the impact of heterogeneities on flow. In their results (reproduced in figure 6c) they also observed the development of anisotropy in the horizontal plane at low sandstone volumes and the approximately log-linear variation of permeability with V_S at high sand proportions. However, the trend observed for vertical flow in their results is different as the effective permeability falls much less rapidly. Since the systems investigated are at different scales (their model dimensions were 0.5 x 0.5 x 0.1m, making them 360 times smaller in volume than the one used in this work) and were constructed differently, this difference is not unexpected; however the similarity in heterogeneity-based variations of horizontal permeability implies that horizontal permeability may be insensitive to scale. At the scale investigated in this work, sandy tidal bar deposits appear to have a much steeper loss of connectivity with reduced sandstone content than observed at the scale used by Ringrose *et al.* (2005) as the mud drapes become more laterally extensive and reduce vertical permeability much faster. Considering the difference in the way the heterogeneities impact on vertical permeability, it is an indication that the REV for horizontal permeability in tidal sandstones is smaller than the REV for vertical permeability. This finding is supported by the work of Jackson *et al.* (2000) and has significance for the utilization of core plug data to characterize tidal sandstones.

Jackson *et al.* (2000) investigated the effectiveness of core-plug data in characterizing the permeability of heterolithic tidal sandstones by studying the impact of sample volume on effective permeability over a range of sandstone/mudstone permeability ratios. Jackson *et al.* studied a range of models varying in size from core plug scale (~30cm^3) to a maximum of approximately 12,000 cm^3 (half the size investigated by Ringrose *et al.*, 2005) They found that no averaging method for core plug permeability data will be representative of heterolithic tidal facies at the reservoir grid block scale regardless of the quantity of the measurements taken and the error introduced by utilizing this data was less for the horizontal than the vertical permeability especially where there is a great contrast in permeability between sand and mudstone (Jackson *et al.* 2000). This observation in combination with result from this work and that of Ringrose *et al.* (2005), further suggest that the core

plug permeability data (especially vertically) will not be representative at the reservoir grid block scale since there is a difference in the results obtained between the scale of Ringrose *et al.* ($0.025m^3$) and that used here ($9m^3$) which are both significantly larger than typical core data but still less than typical reservoir grid block scale ($>100m^3$).

The direction dependent variations in permeability with increased mud drape coverage (heterogeneity-induced isotropy) have potential implications for the development of tidal sandstone reservoirs. This is especially true of reservoirs where sandy tidal bar deposits are the dominant heterogeneities. The implications in fields of generally low permeability such as Linnorm could be significant. Our results indicate that the architecture of the tidal bar deposits produces more obstruction to flow in the dip direction (*x*) yielding an effectively isotropic system.

Based on this, development schemes where the flow is primarily channelled in the strike direction would be advantageous to production in fields with relatively low V_S. Such fields may be especially amenable to targeted line-drive production where the advantage of the higher permeability would reduce the overall cost of developing the field since fewer wells and lower pressure gradients would be required to produce as opposed to situations where flow is primarily in the dip direction.

The onset of anisotropy in the horizontal plane appears to begin within the V_S the same range where the property relationships become log-linear with V_S. This observation could be used to predict reservoir situations where a serious consideration of well positioning and drive direction is warranted. This transition occurs between V_S of 0.75 and 0.8, and implies that in reservoirs with V_S above 0.8, principal drive direction as discussed above may not be such an important consideration and other factors such as drilling costs may take precedence. However, for reservoirs with V_S significantly less than 0.7, the benefits of drive direction may be weighed against other considerations to make optimum decisons.

It is important to note that there the sandy tidal bar blocks in a given reservoir are typically not all oriented in one direction, therefore the orientation of the foresets and toesets of each volume may vary. In cases where an almost random distribution of orientations is present, there will be no advantage in drilling direction as local anisotropy will not be maintained at the field scale and as a result, the benefits may be insignificant. A better understanding of the sandy tidal bar orientation distribution may be merited to take advantage of anisotropy in low V_S reservoirs of significant volumes and accurate property distribution in simulation studies can be used to predict cases where any such benefit exists during reservoir characterization.

The direct correlation of permeability with V_S provides a secondary means of estimating permeability based on estimates of V_S from reservoirs dominated by sandy tidal bar deposits. These effective permeability estimates will be more representative than estimates from conventional log and core data which have consistently been proven to be misleading (Jackson *et al*, 2003) especially for the k_v/k_h ratio which is an especially important parameter for production forecasting in reservoir simulations but is notoriously difficult to predict from conventional wireline data (Brandsaeter *et al*, 2001). Our results present these estimates at a scale that is directly usable in Reservoir simulations and relates to a property that is generally easier to estimate. However, caution must be exercised however in using V_S to characterize the flow properties of reservoir systemssince V_S is not a fixed reservoir property but is also a function of the scale at which it is measured (Ringrose, 2008). This implies that any characterization based on the V_S as defined here might require modification especially when characterizing based on conventional subsurface core-and log-derived measurements of V_S. Effort must be made to ensure that a proper understanding of the variation of V_S with scale for the system being investigated is obtained.

6. CONCLUSIONS

- Direct relationships exist between effective permeability and mudstone coverage. Mudstone coverage can be linked to a more general petrophysical parameter- the net to gross (V_S) for the system using a simple quadratic relationship.
- Permeability reduces significantly in all directions with reduction in V_S. Over the range investigated, k_{nx} reduces by 84% while k_{ny} reduces by 68%. The vertical permeability (k_{nz}) decreases much faster with decreased V_S than in the horizontal plane over the same V_S range as the mud drapes become more laterally extensive. There is a 99% reduction in vertical permeability and the k_{nz}/k_{nh} ratio reduces by a maximum of 96% over the same V_S range.
- The effective permeabilities for this system can be predicted reasonably well using simple polynomial equations and are more representative than estimates from conventional log and core measurements since the relationships have been generated at a scale that significantly closer to the reservoir simulation grid block scale than other data sources.
- Vertical permeability varies more significantly with length scale than horizontal permeability. The correlation of k_v/k_h ratio with V_S is of particular use as it is very poorly estimated by conventional core plug data.
- Local horizontal anisotropy is developed at a V_S of between 0.7 and 0.8 with k_{ny} becoming double k_{nx} at the maximum V_S. This development of horizontal anisotropy observed at low sandstone fractions could have significant impact on production in reservoirs with low V_S. Production schemes where flow is focused in the strike direction may be advantageous compared to production primarily in the dip direction with economic consequences but a greater understanding of the spatial variation of tidal bar orientation is required to predict case where this is significant.
- No transition to effective ‘non-reservoir’ can be observed due to the approach taken to modeling the mud stones where the minimum volumetric V_S is well above documented ‘percolation thresholds’ (0.28 and 0.5).

- The transition to log-linear relationships between effective properties and V_S can be used to define cut-off values. These cut-off values for horizontal and vertical permeability in Linorm are estimated at 0.1mD and 0.02mD respectively. These can be used to generate estimates of NTG.
- V_S is function of scale and thus caution should be exercised when using it to characterize reservoir systems.

7. RECOMMENDATIONS AND FURTHER WORK

- The methodology developed here should be extended to generate multiphase properties using simulations that are analogous to the steady state method used to generate relative permeability data from cores.
- Simulations using the MPFA discussed in section 5.3 should be conducted to investigate the 'grid orientation' errors introduced by the corner-point grid. More accurate effective property results may be obtained using the MPFA in combination with the methodology presented here. This would serve to verify the normalization used and give more confidence and reliability with using the results to characterize tidal sandstones. The 'O' and 'U' MPFA methods have been already been implemented in a commercial simulator (Schlumbergers ECLPISE 300©) and research into utilizing it to verify the work presented here is ongoing. Next generation numerical simulators such as Schlumbergers INTERSECT© currently being developed and tested have also shown promise in handling highly non-orthogonal grids may better resolve the fluid flow fronts distorted by non-orthogonal grid blocks as well as provide more accurate solutions to the equations.
- In this study, the dimensions of the underlying mud drape surfaces were kept uniform. In reality, these surfaces vary in length and alternate realizations in which the range of variability in the shape and scale of the mud drape surfaces are represented should be constructed and simulated to more robustly capture the system behaviors.
- Sandy tidal bars are not the only heterogeneity observed at outcrop and the impact on flow behavior may differ as the heterogeneities interact. A wider range of investigation on the interaction of heterogeneity properties may be warranted.

Nomenclature

Notation

V_S	volumetric sandstone fraction
NTG	Net to gross
MPFA	multipoint flux approximation
q	flowrate
k	permeability
ΔL	linear distance between inlet and outlet measured parallel to flow direction
A	surface area perpendicular to flow direction
m	fraction of mud drape coverage
R^2	goodness of fit
k_v/k_h	ratio of vertical to horizontal permeability
i	grid block number in the x direction
j	grid block number in the y direction
k	grid block number in the z direction

Greek letters

μ	viscosity
$\Delta\theta$	potential

Subscripts

w	phase - water
eff	indicates an effective value for the model
c	indicates potential corrected for depth
eff-0	indicates effective values for a homogenous model
n	normalized value
x	indicates value obtained in x direction
y	indicates value obtained in y direction
z	indicates value obtained in z direction
v	property measured in the vertical direction
h	property measured in the horizontal direction

References

Aavatsmark, I., Barkve, T. Bøe, Ø. and Mannseth, T.: "Discretization on non-orthogonal, quadrilateral Grids for Inhomogeneous, Anisotropic Media" *Journal of computational Physics* (1996) **127** 2-14

Aziz, K.: "Reservoir Simulation Grids: Opportunities and Problems" *SPE Journal of Petroleum Technology* (1993). **25233**

Bagheri M. and Settari A.: "Methods for Modeling Full Tensor Permeability in Reservoir Simulators" *Petroleum Society of Canada* **121** (2003)

Bear, J.: *Dynamics of fluids in porous media*: Elsevier, New York, (1972) 764

Bennion, D. B., Thomas, F. B. and Bietz R. F.: "Low permeability gas reservoirs: problems, opportunities and solutions for drilling, completion, stimulation and production" *SPE* (1996) **35577**

Bown, T. M., and Kraus, M. J.: "Geology and paleoenvironment of the Oligocene Jebel Qatrani formation and adjacent rocks, Fayum depression, Egypt", *U.S. Geological Survey Professional Paper* (1988) **1452**, pp. 1–60

Brandsæter, I., McIlroy, D., Lia, O., Ringrose, P., and Næss, A.: "Reservoir modeling and simulation of Lajas Formation outcrops (Argentina) to constrain tidal reservoirs of the Halten Terrace (Norway)", *Petroleum Geoscience*, (2005): **11**, pp. 37–46

Corbett, P. W. M., and J. L. Jensen.: "Application of probe permeametry to the prediction of two-phase flow performance in laminated sandstones (lower Brent Group, North Sea)": *Marine and Petroleum Geology*, (1991), **10** pp. 335–346.

Ding Y. and Lemmonier P.: "Use of corner point geometry in Reservoir simulation" *SPE* **(**1995) **29933**

Goldthorpe, W. H. and chow, Y. S.: "Unconventional Modeling of Faulted Reservoirs: A Case Study," *SPE* **(**1985) **13526**

Jackson M. D., Hampson G. J. and Sech, R. P.: "Three-dimensional modeling of a shoreface-shelf parasequence reservoir analogue: Part 2. Geologic controls on fluid flow and hydrocarbon recovery", *AAPG Bulletin*, (2009) **93**. 1183 - 1208

Jackson, M. D., and Muggeridge A. H.: "The effect of discontinuous shales on reservoir performance during immiscible flow" *SPE Journal (2000)* **5**, 446–454.

Jackson, M. D., Muggeridge, A. H., Yoshida, S., and Johnson, H. D.: "Upscaling permeability measurements within complex heterolithic tidal sandstones", *Mathematical Geology* (2003), Vol. 35, pp. 499-520

Jackson, M. D., Yoshida, S., Muggeridge, A. H. and Johnson H. D.: "Three-dimensional reservoir characterization and flow simulation of heterolithic tidal sandstones" *AAPG Bulletin* (2005) **89** pp. 507 – 528

Jones, A., Doyle, J., Jacobson, T. and Kjønsvik, D.: "Which sub-seismic heterogeneities influence waterflood performance?" *New Developments in Improved Oil Recovery.* Geological Society, London, Special Publications, In: De Haan, H. J. (ed.) (1995) 84, 5–18.

King, P. R., Buldyrev S. V., Dokholyan N. V., Havlin S., Lee Y., Paul G., Stanley H. E. and Vandesteeg. N.: "Predicting oil recovery using percolation theory": *Petroleum Geoscience* (2001) **7**, p. 105–107.

King, P. R.: "The connectivity and conductivity of overlapping sand bodies" in *North Sea oil and gas reservoirs* II: London, United Kingdom, Graham and Trotman, (1990) p. 353–361. A. T. Buller, E. Berg, O. Hjelmeland, J. Kleppe, O. Torsaeter, and J. O. Aasen, (eds).

Kjønsvik, D., Doyle, J., Jacobsen, T. and Jones, A.: "The effects of sedimentary heterogeneities on production from a shallow marine reservoir – What really matters?" (1994): *SPE* **28445**

Legler B., Johnson H. D., Jackson M. D., Hampson G. J., Jackson C. A-L., El-Barkooky A., Ravnas R., lsop D., and Le Varlet X.: "Characterization of a tide-dominated heterolithic reservoir analogue: the Eocene Dir Abu Lifa Member (Western Desert, Egypt)", *AAPG Annual Convention and Exhibition, Abstracts*. (2010)

Martinius *A. W., Ringrose, P. S., Brostrøm*, C., Elfenbein, C., Næss, A. and Ringås: "Reservoir challenges of heterolithic tidal sandstone reservoirs in the Halten Terrace, mid-Norway" *Petroleum Geoscience* (2005) **11.**

Martinius, A.W., Kaas, I., Næss, A., Helgesen, G., Kjærefjord, J.M. & Leith, D.A.: "Sedimentology of the heterolithic and tide-dominated Tilje Formation (Early Jurassic, Halten Terrace, offshore mid-Norway)". In: Martinsen, O.J. & Dreyer, T. (eds) *Sedimentary Environments Offshore Norway – Paleozoic to Recent. Norwegian Petroleum Society, Special Publications,* (2001) **10** pp103–144.

Massart B.Y.G. et al. "Three-dimensional Characterization and Surface-based Modeling of Tide-dominated Heterolithic Sandstones" Paper presented at the 2011 *EAGE* conference, Vienna, May.

Nio, S. D., and Yang, C.S.: "Diagnostic Attributes of Clastic Tidal Deposits: a Review", *Clastic Tidal Sedimentology*, Canadian Society of Petroleum Geologists (1991) **16**, pp. 3-28

Norris, R. J., and J. J. M. Lewis.: "The geological modeling of effective permeability in complex heterolithic facies: *Society of Petroleum Engineers Journal* (1991) **22692**.

Oost, A. P., and J. H. Baas.: "The development of small scale bedforms in tidal environments: An empirical model for unsteady flow and its applications": *Sedimentology* (1994) 41, pp. 883– 903.

Peaceman D. W.: "Calculation of Transmissibilities of Gridblocks Defined by Arbitrary Corner Point Geometry" *SPE* **37306 (**1996)

Reineck, H.E. and Wunderlich, F.: "Classification and origin of flaser and lenticular bedding". *Sedimentology* (1968) **11**: pp 99-104.

Renard Ph. and de Marsily G.: "Calculating equivalent permeability: a review" Advances in water resources (1997) **20** 253-278

Ringrose P. S., Skjetne E., and Elfenbein C.: "Permeability Estimation Functions Based on Forward Modeling of Sedimentary Heterogeneity" *SPE* (2003) **84275**

Ringrose, P. S. "Total Property Modeling: Dispelling the Net-to-Gross myth" *SPE* (2008) **106620**

Ringrose, P. S., Nordhal, K., and Wen, R.: "Vertical Permeability Estimation of Heterolithic Tidal Deltaic Sandstones", *Petroleum Geoscience*, (2005) **11.** 29-36

Sech, R. P., Jackson M. D. and Hampson G. J.: "Three-dimensional modeling of a shoreface-shelf parasequence reservoir analogue: Part 1. Surface-based modeling to capture high-resolution facies architecture", *AAPG Bulletin*, (2009) **93.** 1155 - 1181

Todd, M. R., O'Dell P. M. and Hirasaki G.J.: "Methods for Increased Accuracy in Numerical Reservoir Simulators" *SPE* (1972) **3516**

Wadsley, W. A.: "Modeling Reservoir Geometry with Non-Rectangular Coordinate Grids," *SPE* (1980) **9369**

Warren, J. E., and Price, H. S.: "Flow in heterogeneous porous media": *SPE Journal* (1961). **1** 153–169.

White, C. D., and Barton, M. D.: "Comparison of the recovery behavior of contrasting reservoir analogues in the Ferron Sandstone using outcrop studies and numerical simulation" *Report of investigations n°249, Bureau of Economic Geology, the University of Texas at Austin* (1999)

Willis, B. J. and White C. D.: "Quantitative Outcrop Data for Flow Simulation", *Journal of Sedimentary Research*, (2000) **70.** 788 - 802

Wu, X. H. and Parashkevov, R. R.: "Effect of Grid Deviation on Flow solutions" *SPE* **(**2005) **92868**

APPENDICES

Appendix A – Literature Reviews

SPE Journal, (1961) 1579-G.

Flow in heterogeneous porous media

Authors: Warren, J. E., and Price, H. S.

Contribution: Studied the effect of the disposition of heterogeneous permeabilities on single phase flow in for a known permeability distribution function using numerical computations. Established a consistent and logical methodology (the 'sealed side' pressure solver) for calculating effective permeability in heterogeneous systems

Methodology: Flow simulation of random heterogeneous three-dimensional arrays made up of homogenous porous blocks. Each element of the box was assigned permeabilities according to specific distribution functions and anisotropy by varying the block sizes. The effective permeability was calculated between two equipotential surfaces after steady state was reached using the standard Darcy flow equation. .

Conclusions:

1. The most probable behaviour of a heterogeneous system in single phase flow approaches the geometric mean of the individual permeabilities and the flow geometry and anisotropy do not significantly affect this value
2. The permeability determined from a pressure build-up test gives a reasonable value for the effective permeability in the drainage area.
3. Measures of the degree of heterogeneity may be inferred from core and well test data.

Comments: They assumed that core and well test data adequately represent reservoir characteristic. Subsequent work has invalidated these assumptions and core data has been show to be inadequate in describing many heterogeneous systems

***SPE* (1980) 9369**

Modeling Reservoir Geometry with Non-Rectangular Coordinate Grids

Author: Wadsley, W. A.

Contribution: Describes a practical and routine method for using non-rectangular grids in reservoir simulation and illustrates the situations in which these grids may be beneficial and the advantages of using these grids for heterogeneous systems.

Methodology: Derives a series of finite difference equations adapted to non-rectangular grids and equations are based on curvilinear systems

Conclusions:

1. Corner point grids are advantageous when reservoir boundaries are faulted; systems are anisotropic and/or have varying thickness and dip.
2. Presents a systems for calculation of interblock transmissibilties
3. These systems can be used for study of well performance by changing the grid systems
4. The results of these grids is as good or better than Cartesian grids and easy to construct

Comments: Good description of Corner-point grid methodology, not enough description of the errors introduced by non-orthogonality.

U.S. Geological Survey Professional Paper (1988) 1452

Geology and paleoenvironment of the Oligocene Jebel Qatrani formation and adjacent rocks, Fayum depression, Egypt

Authors: Bown, T. M., and Kraus, M. J.

Contribution: Geological description and classification of the heterolithic tidal sandstone facies in the Dir Abu Lifa outcrop member.

Methodology: Geological surveys

Conclusions: The Dir Abu Lifa member was subdivided into 8 units with a diversity of lithologies which correspond to small variations of the depositional environment.

Comments: Provides a detailed description of depositional environments for the analogue used for the model used in this work and a detailed description of the sandy tidal bar heterogeneity.

North Sea Oil and Gas Reservoirs II (1990)

The Connectivity and Conductivity of Overlapping Sand Bodies

Author: King, P. R.

Contribution to the understanding Impact of heterogeneity on flow in wave dominated shallow marine reservoirs

Simple modelling of connectivity in a sand and shale in a reservoir.

Objective of the paper:

Explain generic behaviour of connectivity and conductivity of uncorrelated, overlapping sand bodies using simple theory.

Methodology:

Percolation theory.

Conclusions :

For simple model of sand bodies it is possible to model the connectivity behaviour at any scale by using percolation theory. Curves for connected sand fraction and effective permeability as a function of Net-to-Gross ratio and well spacing were generated.

Comments:

Makes use of simple geometric shapes (rectangles) to represent sand bodies and assumes connectivity between sand bodies in contact. Percolation theory however is only strictly accurate near the threshold and will not give accurate otherwise.

Journal of Computational Physics 127 2 -14 **(1996)**

Discretization on non-orthogonal, quadrilateral Grids for Inhomogeneous, Anisotropic Media

Authors: Aavatsmark, I., Barkve, T. Bøe, Ø. and Mannseth, T.

Contribution: Introduced and derived two of the most common classes of discretization methods (Multipoint Flux Approximations) for reducing the error introduced by non-orthogonality of simulation grids and applied the concept to curvilinear grids.

Objective: To give a detailed presentation of the discretization methods developed by the authors and apply them to a specific case of irregular quadrilateral grids - non-orthogonal curvilinear grids.

Methodology: The methods were derived from basic model equations for multi-phase flow in porous media. These equations are discretized using the Control-volume formulation.

Conclusions: Presented the formulation of discretization methods and described the O and U methods as a means of handling non-orthogonal quadrilateral grids. Describes the ability of the both methods to handle media inhomogeniety, anisotropy and grid non-orthogonality. Demonstrated the improved accuracy of the methods as opposed to standard schemes and described cases where the methods provide different solutions and a hybrid of both methods may be advantageous.

Comments: Clear and concise introduction to the MPFA methods.

Mathematical Geology (2003), Vol. 35

Upscaling permeability measurements within complex heterolithic tidal sandstones

Authors: Jackson, M. D., Muggeridge, A. H., Yoshida, S., and Johnson, H. D

Contribution: Investigated the effect of sample size on the effective permeability of heterolithic tidal sandstones and established that effective permeability values vary as a function of sample volume.

Methodology: Flow simulation using 3-dimensional models reconstructed directly from rock specimens ~0.02m^3 using serial sectioning techniques together with surface mapping software.

Conclusions: Found that both individual and averaged effective permeability values are a function of the sample volume at which they are measured and permeability data obtained from core-plugs will not be representative at the scale of a reservoir model grid-block regardless of the number of measurements taken. The variation if permeability with scale was found to be more significant vertically than horizontally. They also found that the error introduced by using averaged data may be minimized using the appropriate averaging scheme for a given facies type and flow direction.

Comments: Sample volumes investigated are still significantly smaller than typical reservoir grid block volumes

***SPE* (2003) 84275**

Permeability Estimation Functions Based on Forward Modeling of Sedimentary Heterogeneity

Authors: Ringrose P. S., Skjetne E. and Elfenbein C.

Contribution: Used stochastic models of 3D heterogeneity at the 10cm – 10m scale to establish a series of functional relationships between effective permeability, bedding type and sand volume fraction.

Methodology: Built a 3D model from equations which approximate the geometrical arrangement of sedimentary bedding by migrating a set of bedding surfaces to mimic sedimentation. Used flow simulation methodology of Warren and Price (1961), to generate effective permeabilities.

Conclusions: Found that traditional averages of permeability do not realistically describe permeability of heterogeneous facies. The upscaled permeability will depend on the flow regime of the system which they describe as being: Sand dominated, Percolation and mud dominated flow regimes. These regimes were found to be dependent on the specific formation and flow direction.

Comments: Arrives at similar conclusions with Jackson et al. 2005, using a different methodology. .

Petroleum Geoscience 11 (2005)

Reservoir challenges of heterolithic tidal sandstone reservoirs in the Halten Terrace, mid-Norway

Authors: Martinius A. W., Ringrose, P. S., Brostrøm, C., Elfenbein, C., Næss, A. and Ringås, J. E.

Contribution: A presents a comprehensive overview of the geological setting and reservoir characteristics of the Halten terrace reservoirs and highlights the main challenges encountered when developing these reservoirs.

Objective: To provide a concise overview of the heterolithic tidal sandstone reservoirs of the Halten terrace and serve as an introduction to discussions on the characterization and modeling of these reservoirs.

Methodology: The summary discussion is based on a wide range of data from fields in the region, including log and core data as well as outcrop observations.
.
Conclusions: Fields are described and classified based on three main types of heterogeneity: (1) heterolithic facies, (2) faulting and (3) diagenesis. The challenges are discussed according to the field setting: shallow (1–3 km burial depth), deep (3–5 km) or very deep (currently up to 5.6 km) and major heterogeneity.

Comments: Provides a good summary of the challenges encountered with heterolithic tidal sandstone reservoirs in the Halten Terrace, Norway

Petroleum Geoscience, (2005) 11.

Vertical Permeability Estimation of Heterolithic Tidal Deltaic Sandstones

Authors: Ringrose, P. S., Nordhal, K., and Wen, R

Contribution: Proposed a method for estimation of vertical permeability in heterolithic tidal deltaic sandstones based on flow simulation of $0.025m^3$, 3-dimensional stochastic, process-based models of sedimentary bedding.

Methodology: 3D models were built from equations which approximate the geometrical arrangement of sedimentary bedding and mimic sedimentation processes similar to that previously established by Ringrose et al. (2003). Flow simulation was performed using the methodology of Warren and Price (1961), to generate effective permeabilities.

Conclusions: Found that the process-based modelling approach allows tidal depositional systems to be quantified in terms of effective properties. The general functions fitted to stochastic simulations of effective permeability of a large number of sedimentary bedding models provide are promising as predictive tools for reservoir characterization especially valuable for estimating vertical permeability.

Comments: Their model is at a scale which is much smaller than typical reservoir gridblock scales.

AAPG Bulletin (2005) 89

Three-dimensional reservoir characterization and flow simulation of heterolithic tidal sandstones

Authors: Jackson, M. D., Muggeridge, A. H., Yoshida, S., and Johnson, H. D

Contribution: Characterized the sandstone connectivity, effective permeability, and displacement efficiency of heterolithic tidal sandstones

Objective: To present a methodology for reconstructing the complex, three-dimensional (3-D) architecture of heterolithic tidal intervals directly from outcrop data, calculate the connectivity of sands, effective permeability, and displacement efficiency of each rock specimen model. The paper also compared sand connectivity in 2 and 3 dimensions to verify the usefulness of 2D models in predicting reservoir properties and explains why intervals of low net to gross usual produce large hydrocarbon volumes.

Methodology: Flow simulation of 3-dimensional models reconstructed directly from rock specimens ~0.075m^3 using serial sectioning techniques and surface mapping software. Simulations to yield effective permeability were performed using the sealed side pressure solver method of Warren and Price (1961).

Conclusions:

1. Found that that the key control on reservoir quality is the connectivity and continuity of the sandstone and mudstone layers.
2. If sandstone layers are connected, they are likely to be productive even at low values of net-to-gross (about 0.3–0.5).
3. Measurements of sandstone connectivity in 2-D underestimate true value.
4. Low to moderate net-to-gross heterolithic tidal sandstones may be very productive since they are well connected in 3-D, with high horizontal permeabilities and sweep efficiencies but low vertical permeabilities.
5. Verified that connectivity in 2D is generally less than connectivity in 3D and that no number of core plug measurements provides representative values of permeability

Comments: Model size investigated is significantly smaller than typical reservoir grid block volumes (models used in this study ranged from core–scale to a maximum of 0.5 x 0.5 x 0.3m). Results may still not be fully representative at that scale.

Paper presented at the 2011 *EAGE* conference, Vienna, May.

Three-dimensional Characterization and Surface-based Modeling of Tide-dominated Heterolithic Sandstones

Authors: Massart B. Y. G. et al.

Contribution: Describes the details and construction of the model ($9m^3$) used for flow simulation in this work

Methodology: The 3-D high resolution model of sandy tidal bar deposits was built using surface-based modeling techniques adapted to for 3-D flow simulation and based on observations and measurements of details from the Dir Abu Lifa outcrop member (Western Desert, Egypt) as an analogue for the Linnorm field.

Conclusions: Data were collected at different localities to extract the geometrical parameters required to reproduce the heterogeneity-defining surfaces. The deposits at the Gecko Nose locality correspond to sandy tidal bar deposits and thus Statistics on the dimensions of cross-bed sets and the corresponding best-fit ellipsoid building volumes were extracted from there. The building volumes were chosen as ellipsoids to fit the elliptical erosive bases of the cross-bed sets and a generic function was determined to model the geometry of the foresets and reproduce their curvature. A frequency function of mud drape along the foresets was also defined to reproduce the mud drape distribution along foresets

Comments: The model created is the largest scale model of heterolithic tidal sandstones created to be used for extracting flow properties found in the literature.

Appendix B – Milestones Table

Table B1 - Milestones in the Impact of heterogeneity on production in heterolithic Tidal sandstones: Application to the Linnorm field, offshore Norway.

Paper No.	Year of Publication	Title	Authors	Contribution
SPE 1579-G	1961	"Flow in heterogeneous porous media"	Warren, J. E., and Price H.S	Established a consistent and logical methodology (the 'sealed side' pressure solver) for calculating effective permeability in heterogeneous systems
SPE (1980) 9369	1980	"Modeling Reservoir Geometry with Non-Rectangular Coordinate Grids"	Wadsley, W. A.	Describes a practical and routine method for using non-rectangular grids in reservoir simulation and illustrates the situations in which these grids may be beneficial and the advantages of using these grids for heterogeneous systems
USGS Professional paper 1452	1988	"Geology and paleoenvironment of the Oligocene Jebel Qatrani formation and adjacent rocks, Fayum depression, Egypt"	Bown, T. M., and Kraus, M. J.	Provides a Geological description and classification of the heterolithic tidal sandstone facies in the Dir Abu Lifa outcrop member which are used as an analogue to the Linnorm field
North Sea Oil and Gas Reservoirs II	1990	The Connectivity and Conductivity of Overlapping Sand Bodies.	P. R., King.	Simple modelling of connectivity in a sand and shale in a reservoir and connectivity based on percolation theory.
SPE (1995) 29933	1995	"Use of corner point geometry in Reservoir simulation"	Ding Y. and Lemmonier P.	Presents a technique for maintaining accuracy of fluid flow equations with different control volume type approximations when using corner point grids to describe heterogeneous systems and discusses its application range based on test case results.
Journal of Computational Physics 127	1996	" Discretization on non-orthogonal, quadrilateral Grids for Inhomogeneous, Anisotropic Media"	Aavatsmark, I., Barkve, T. Bøe, Ø. and Mannseth, T.	Introduced and derived two of the most common classes of discretization methods (Multipoint Flux Approximations) for reducing the error introduced by non-orthogonality of simulation grids and applied the concept to curvilinear grids.
Mathematical Geology 35	2003	" Upscaling permeability measurements within complex heterolithic tidal sandstones"	Jackson, M. D., Muggeridge, A. H., Yoshida, S., and Johnson, H. D.	Investigated the effect of sample size on the effective permeability of heterolithic tidal sandstones and established that effective permeability values vary as a function of sample volume
SPE 84275	2003	" Permeability Estimation Functions Based on Forward Modeling of Sedimentary Heterogeneity"	Ringrose P. S., Skjetne E. and Elfenbein C.	Used stochastic models of 3D heterogeneity at the 10cm – 10m scale to establish a series of functional relationships between effective permeability, bedding type and sand volume fraction
Petroleum Geoscience 11	2005	"Reservoir challenges of heterolithic tidal sandstone reservoirs in the Halten Terrace, mid-Norway"	Martinius A. W., Ringrose, P. S., Brostrøm, C., Elfenbein, C., Næss, A. and Ringås, J. E.	Presents a comprehensive summary of the geological setting and reservoir characteristics of the Halten terrace reservoirs and highlights the main challenges encountered when developing these reservoirs.
Petroleum Geoscience 11	2005	"Vertical Permeability Estimation of Heterolithic Tidal Deltaic Sandstones"	Ringrose, P. S., Nordhal, K., and Wen, R.	Proposed a method for estimation of vertical permeability in heterolithic tidal deltaic sandstones based on flow simulation of 0.025m3, 3-dimensional stochastic, process-based models of sedimentary bedding.
AAPG Bulletin 89	2005	"Three-dimensional reservoir characterization and flow simulation of heterolithic tidal sandstones"	Jackson, M. D., Muggeridge, A. H., Yoshida, S., and Johnson, H. D	Characterized the sandstone connectivity, effective permeability, and displacement efficiency of heterolithic tidal sandstones and their impact on flow properties using flow simulation of reconstructed rock samples
Paper presented at the 2011 EAGE conference, Vienna, May.	2011	Three-dimensional Characterization and Surface-based Modeling of Tide-dominated Heterolithic Sandstones"	Massart B. Y. G.	Describes the details of construction of the model used for flow simulation in this work

Appendix C – Sample simulation DATA files

C1 – Generic simulation DATA file for X-permeability calculation.

```
-- RUNSPEC SECTION ================================================

RUNSPEC

TITLE
  X-permeability Simulation

CART

-- Grid dimensions
DIMENS
-- Nx   Ny   Nz
 100   100   988 /

-- Dead oil Model used, phases are oil and water
WATER
OIL

-- Note LAB units are used throughout .DATA file
LAB

START
  01 'Jan' 2011 /

WELLDIMS
-- NWMAX NWMAXZ NGMAX NWGMAX
  200    988     2    200 /

TABDIMS
-- NTSFUN   NTPVT    NSSFUN NPPVT
           1     1     100    100 /

TRACERS
   0    1    0    0 'NODIFF' /

-- Format output grid file

FMTOUT

NSTACK
-1 /

MESSAGES
  1000   1000   1000   1000   1000   1000   1000   1000   1000   1000   /

-- Unified format
UNIFOUT

-- GRID SECTION ===================================================

GRID

-- Use NEWTRAN for irregular grids and OLDTRAN for Cartesian grids
NEWTRAN
```

```
--Switch off output to the PRT file during grid loading to reduce output PRT file size
NOECHO

--Include file grid file
INCLUDE
 'Gridmodel1blanked.grdecl' /

INCLUDE
  'Gridmodel1blank2.ACTNUM.INC' /

-- Give All Cells Same Porosity
PORO
9880000*0.3 /

--Include PERMX file for the specific case. Number at the end of filename indicates the % mud drape coverage for that case
INCLUDE
'TransmissibilityModel1Muddrapes20.grdecl' /

--make each grid block isotropic
COPY
'PERMX' 'PERMY' /
'PERMX' 'PERMZ' /
/

--Define Buffer Layers with high Perm at the extreme ends of the grid for the specific orientation (X in this case)
BOX
1 1 1 100 1 988 /

EQUALS
'PERMX' 54000000 /
/

COPY
'PERMX' 'PERMY' /
'PERMX' 'PERMZ' /
/

ENDBOX

BOX
100 100 1 100 1 988 /

EQUALS
'PERMX' 54000000 /
/

COPY
'PERMX' 'PERMY' /
'PERMX' 'PERMZ' /
/

ENDBOX

-- Set up NNC's across pinched-out cells
PINCH
0.000001 'GAP' /

-- Produce initial file for GRAF
```

```
INIT

-- OUTPUT GRID
GRIDFILE
1 1 /

-- PROPERTIES SECTION  ============================================

PROPS

-- oil/water relative permeability and capillary pressure table (not used here since it is single phase)
--    Sw      Krw      Kro       Pcow
SWOF
           0         0                  1                  0
           0.485     0.000253906        0.1771875          0
           0.5186    0.00101752         0.112846278        0
           0.527     0.001365569        0.0999635          0
           0.5354    0.001802943        0.088216582        0
           0.5942    0.008970657        0.032282886        0
           0.6698    0.040664815        0.005171718        0
           0.7034    0.070376388        0.00156711         0
           0.7622    0.162248358        3.67416E-05        0
           0.8       0.26               0                  0
           1         1                  0                  0 /

-- Specify fluid properties
--        OIL      WATER      GAS
--      (g/cc)   (g/cc)   (g/cc)
DENSITY
        0.625     0.978      0.0/

-- Tracer names and their associated stock tank phases are defined using the tracer keyword

TRACER
 'DYE' 'WAT' /
/

-- Specify rock properties
--     REF.PRES   ROCK-COMPRESSIBILITY
--      (BAR)         (1/BAR)
ROCK
        2.00       0.000000145  /

-- Dead oil PVT table (FVF and Viscosity must vary with pressure)
--    Oil phase press.   Oil FVF   Oil Viscosity
--        (BAR)        ()    (CPoise)
PVDO
          0.4137       1.09    0.2900
          1.379       1.08    0.2901
          1.6547      1.07    0.2902
          1.9305      1.06    0.2903
          2.2063      1.05    0.2904
          2.4821      1.04    0.2905
          2.7579      1.03    0.2906
          3.0337      1.02    0.2907
          3.3095      1.01    0.2908
          4.5          1.009   0.2909
          6.11         1.008   0.2910
           8.4         1.007   0.2911        /
```

```
-- Water PVT table
--    Ref. press.  FVF-WATER  Compressibility  Viscosity  Viscosibility
--     (BAR)       ()      (1/BAR)     (CPoise)      (1/BAR)
PVTW
      2.00         1.0         0.00         0.31         0.0  /

--  REGIONS SECTION ================================================

REGIONS

-- SOLUTION SECTION ================================================

SOLUTION

EQUIL
-- for single phase water cases, equilibrate model by stting OWC at the tiop of or above the model dimensions
-- DATUM     PRESSURE     DEPTH     OWC     DEPTH     GOC     INIT    INIT    INTE
-- DEPTH     @ DATUM      OWC       CAP     GOC       CAP     TYPE    TYPE    N
--                          PRESS           PRE     LO      DO
  100       2.00        100      0.0    /

--Tracer concentrations
TVDPFDYE
100.0   0.0
100.0   0.0  /
/

-- SUMMARY SECTION ================================================================

SUMMARY

-- Specify creation of summary file
RPTSMRY
  1 /

RUNSUM

-- Specify output of oil and water in place to summary file
FOIP
FWIP
-- output liquid, oil,water production rate
FLPR
FOPR
FWPR
-- output field pressure
FPR
-- output water injection rate
FWIR
-- output well pressures
WBP5
FTPRDYE
FTPTDYE
/

-- SCHEDULE SECTION ================================================================

SCHEDULE

RPTRST
POT /
```

```
-- Include file containing WELSPECS, WCONPROD and WCONINJE keywords
INCLUDE
  'welspecsa.ecl' /

WPAVE
1.0 0.5 /

-- Specify performance of solver (requirements vary for each case)

TUNING
0.1 1.5              /
                     /
2* 200 1* 4          /

NUPCOL
15 /

ECHO

--time to reach steady state id short. Simualtions for as low as 2 hrs were used. Some were simulated longer
TSTEP
10*0.2 /

RPTSCHED
'RESTART = 1' 'FIPTR=2' /

END
```

Welspecs file

```
-- Injecting water into each grid block to impose linear, 1-directional flow
--
WELSPECS
 'INJ  1' 'INJ'  1   1 -1 'WATER' -1 /
 'INJ  2' 'INJ'  1   2 -1 'WATER' -1 /
 'INJ  3' 'INJ'  1   3 -1 'WATER' -1 /
    .       .    .   .  .      .       .
    .       .    .   .  .      .       .
    .       .    .   .  .      .       .
    .       .    .   .  .      .       .
    .       .    .   .  .      .       .
    .       .    .   .  .      .       .
    .       .    .   .  .      .       .
    .       .    .   .  .      .       .
  'INJ 97' 'INJ'  1  97 -1 'WATER' -1 /
 'INJ 98' 'INJ'  1  98 -1 'WATER' -1 /
 'INJ 99' 'INJ'  1  99 -1 'WATER' -1 /
 'INJ100' 'INJ'  1 100 -1 'WATER' -1 /
 'PROD  1' 'PROD' 100   1 -1 'WATER' -1 /
 'PROD  2' 'PROD' 100   2 -1 'WATER' -1 /
 'PROD  3' 'PROD' 100   3 -1 'WATER' -1 /
    .       .    .   .  .      .       .
    .       .    .   .  .      .       .
    .       .    .   .  .      .       .
```

```
    .       .   .   .  .      .       .
    .       .   .   .  .      .       .
    .       .   .   .  .      .       .
    .       .   .   .  .      .       .
    .       .   .   .  .      .       .
 'PROD 97' 'PROD' 100  97 -1 'WATER' -1 /
 'PROD 98' 'PROD' 100  98 -1 'WATER' -1 /
 'PROD 99' 'PROD' 100  99 -1 'WATER' -1 /
 'PROD100' 'PROD' 100 100 -1 'WATER' -1 /
/
--completions data for the wells

COMPDAT
 'INJ  1'  1   1 1   988 'OPEN' -1 1 /
 'INJ  2'  1   2 1   988 'OPEN' -1 1 /
 'INJ  3'  1   3 1   988 'OPEN' -1 1 /
    .       .   .   .  .      .       .
    .       .   .   .  .      .       .
    .       .   .   .  .      .       .
    .       .   .   .  .      .       .
    .       .   .   .  .      .       .
    .       .   .   .  .      .       .
    .       .   .   .  .      .       .
    .       .   .   .  .      .       .
 'INJ 97'  1  97 1   988 'OPEN' -1 1 /
 'INJ 98'  1  98 1   988 'OPEN' -1 1 /
 'INJ 99'  1  99 1   988 'OPEN' -1 1 /
 'INJ100'  1 100 1   988 'OPEN' -1 1 /
 'PROD  1' 100   1 1   988 'OPEN' -1 1 /
 'PROD  2' 100   2 1   988 'OPEN' -1 1 /
 'PROD  3' 100   3 1   988 'OPEN' -1 1 /
    .       .   .   .  .      .       .
    .       .   .   .  .      .       .
    .       .   .   .  .      .       .
    .       .   .   .  .      .       .
    .       .   .   .  .      .       .
    .       .   .   .  .      .       .
    .       .   .   .  .      .       .
    .       .   .   .  .      .       .
 'PROD 97' 100  97 1   988 'OPEN' -1 1 /
 'PROD 98' 100  98 1   988 'OPEN' -1 1 /
 'PROD 99' 100  99 1   988 'OPEN' -1 1 /
 'PROD100' 100 100 1   988 'OPEN' -1 1 /
/
--Injection rates and controls – rates are made equal
WCONINJE
 'INJ*'  'WATER' 'OPEN' 'RATE'   50  1.0E20  8.4 /
/

WCONPROD
 'PROD*'  'OPEN' 'LRAT' 1.0E20 1.0E20  1.0E20   50  1.0E20  1 /
/
```

```
--tracer injection to observe flow path
WTRACER
'INJ  1'   'DYE'    1          /
'INJ  2'   'DYE'    1          /
'INJ  3'   'DYE'    1          /
     .        .    .    .  .       .
     .        .    .    .  .       .
     .        .    .    .  .       .
     .        .    .    .  .       .
     .        .    .    .  .       .
     .        .    .    .  .       .
     .        .    .    .  .       .
     .        .    .    .  .       .
'INJ 97'   'DYE'    1          /
'INJ 98'   'DYE'    1          /
'INJ 99'   'DYE'    1          /
'INJ100'   'DYE'    1          /
/
```

C2 – Generic simulation DATA file for Y-permeability calculation.

```
-- RUNSPEC SECTION ================================================

RUNSPEC

TITLE
  Y-permeability Simulation

CART

-- Grid dimensions
DIMENS
-- Nx   Ny   Nz
 100   100   988 /

-- Dead oil Model used, phases are oil and water
WATER
OIL

-- Note LAB units are used throughout .DATA file
LAB

START
  01 'jan' 2011 /

WELLDIMS
-- NWMAX NWMAXZ NGMAX NWGMAX
  200    988     2    200 /

TABDIMS
-- NTSFUN   NTPVT    NSSFUN NPPVT
           1      1     100    100 /

TRACERS
   0    1    0    0 'NODIFF' /

-- Format output grid file

FMTOUT

NSTACK
-1 /

MESSAGES
  1000   1000   1000   1000   1000   1000   1000   1000   1000   1000   /

-- Unified format
UNIFOUT

-- GRID SECTION ===================================================

GRID

-- Use NEWTRAN for irregular grids and OLDTRAN for Cartesian grids
NEWTRAN
```

```
--Switch off output to the PRT file during grid loading to reduce output PRT file size
NOECHO

--Include file grid file
INCLUDE
 'Gridmodel1blanked.grdecl' /

INCLUDE
  'Gridmodel1blank2.ACTNUM.INC' /

-- Give All Cells Same Porosity
PORO
9880000*0.3 /

--Include PERMX file for the specific case. Number at the end of filename indicates the % mud drape coverage for that case
INCLUDE
'TransmissibilityModel1Muddrapes20.grdecl' /

--make each grid block isotropic
COPY
'PERMX' 'PERMY' /
'PERMX' 'PERMZ' /
/

--Define Buffer Layers with high Perm at the extreme ends of the grid for the specific orientation (Y in this case)
BOX
1 100 1 1 1 988 /

EQUALS
'PERMX' 54000000 /
/

COPY
'PERMX' 'PERMY' /
'PERMX' 'PERMZ' /
/

ENDBOX

BOX
1 100 100 100 1 988 /

EQUALS
'PERMX' 54000000 /
/

COPY
'PERMX' 'PERMY' /
'PERMX' 'PERMZ' /
/

ENDBOX

-- Set up NNC's across pinched-out cells
PINCH
0.000001 'GAP' /

-- Produce initial file for GRAF
INIT
```

```
-- OUTPUT GRID
GRIDFILE
1 1 /

-- PROPERTIES SECTION  ============================================

PROPS

-- oil/water relative permeability and capillary pressure table (not used here since it is single phase)
--    Sw      Krw      Kro       Pcow
SWOF
          0         0                  1                  0
          0.485     0.000253906        0.1771875          0
          0.5186    0.00101752         0.112846278        0
          0.527     0.001365569        0.0999635          0
          0.5354    0.001802943        0.088216582        0
          0.5942    0.008970657        0.032282886        0
          0.6698    0.040664815        0.005171718        0
          0.7034    0.070376388        0.00156711         0
          0.7622    0.162248358        3.67416E-05        0
          0.8       0.26               0                  0
          1         1                  0                  0 /

-- Specify fluid properties
--        OIL      WATER      GAS
--     (g/cc)   (g/cc)   (g/cc)
DENSITY
        0.625     0.978      0.0/

-- Tracer names and their associated stock tank phases are defined using the tracer keyword

TRACER
 'DYE' 'WAT' /
/

-- Specify rock properties
--     REF.PRES   ROCK-COMPRESSIBILITY
--      (BAR)         (1/BAR)
ROCK
        2.00       0.000000145  /

-- Dead oil PVT table (FVF and Viscosity must vary with pressure)
--    Oil phase press.   Oil FVF   Oil Viscosity
--        (BAR)        ()    (CPoise)
PVDO
          0.4137      1.09    0.2900
          1.379       1.08    0.2901
          1.6547      1.07    0.2902
          1.9305      1.06    0.2903
          2.2063      1.05    0.2904
          2.4821      1.04    0.2905
          2.7579      1.03    0.2906
          3.0337      1.02    0.2907
          3.3095      1.01    0.2908
          4.5          1.009   0.2909
          6.11         1.008   0.2910
           8.4         1.007   0.2911       /

-- Water PVT table
--    Ref. press.  FVF-WATER  Compressibility  Viscosity  Viscosibility
```

```
--    (BAR)      ()     (1/BAR)     (CPoise)      (1/BAR)
PVTW
      2.00         1.0         0.00         0.31         0.0  /

--  REGIONS SECTION ====================================================

REGIONS

-- SOLUTION SECTION ====================================================

SOLUTION

EQUIL
-- for single phase water cases, equilibrate model by stting OWC at the tiop of or above the model dimensions
-- DATUM     PRESSURE     DEPTH     OWC     DEPTH     GOC     INIT    INIT    INTE
-- DEPTH     @ DATUM      OWC       CAP     GOC       CAP     TYPE    TYPE    N
--                        PRESS             PRE     LO      DO
  100       2.00        100       0.0    /

--Tracer concentrations
TVDPFDYE
100.0   0.0
100.0   0.0  /
/

-- SUMMARY SECTION ==============================================================

SUMMARY

-- Specify creation of summary file
RPTSMRY
  1 /

RUNSUM

-- Specify output of oil and water in place to summary file
FOIP
FWIP
-- output liquid, oil,water production rate
FLPR
FOPR
FWPR
-- output field pressure
FPR
-- output water injection rate
FWIR
-- output well pressures
WBP5
FTPRDYE
FTPTDYE
/

-- SCHEDULE SECTION ============================================================

SCHEDULE

RPTRST
POT /

-- Include file containing WELSPECS, WCONPROD and WCONINJE keywords
```

```
INCLUDE
  'welspecsa.ecl' /

WPAVE
1.0 0.5 /

-- Specify performance of solver (requirements vary for each case)

TUNING
0.1 1.5              /
                     /
2* 200 1* 4          /

NUPCOL
15 /

ECHO

--time to reach steady state id short. Simualtions for as low as 2 hrs were used. Some were simulated longer
TSTEP
10*0.2 /

RPTSCHED
'RESTART = 1' 'FIPTR=2' /

END
```

Welspecs file for Y perm

```
--
WELSPECS
   'INJ 1'   'INJ'  1  1  -1  'WATER'  -1 /
   'INJ 2'  'INJ'  2  1  -1  'WATER'  -1 /
   'INJ 3'  'INJ'  3  1  -1  'WATER'  -1 /
    .        .    .   .  .       .        .
    .        .    .   .  .       .        .
    .        .    .   .  .       .        .
    .        .    .   .  .       .        .
    .        .    .   .  .       .        .
    .        .    .   .  .       .        .
    .        .    .   .  .       .        .
    .        .    .   .  .       .        .
   'INJ 97'  'INJ'  97  1  -1  'WATER'  -1 /
   'INJ 98'  'INJ'  98  1  -1  'WATER'  -1 /
   'INJ 99'  'INJ'  99  1  -1  'WATER'  -1 /
   'INJ100'  'INJ'  100  1  -1  'WATER'  -1 /
    'PROD  1'  'PROD'  1  100  -1  'WATER'  -1 /
    'PROD  2'  'PROD'  2  100  -1  'WATER'  -1 /
    'PROD  3'  'PROD'  3  100  -1  'WATER'  -1 /
    .        .    .   .  .       .        .
    .        .    .   .  .       .        .
    .        .    .   .  .       .        .
    .        .    .   .  .       .        .
    .        .    .   .  .       .        .
    .        .    .   .  .       .        .
```

```
    .       .   .   .   .      .       .
    .       .   .   .   .      .       .
   'PROD 97'  'PROD'  97  100  -1  'WATER'  -1 /
   'PROD 98'  'PROD'  98  100  -1  'WATER'  -1 /
   'PROD 99'  'PROD'  99  100  -1  'WATER'  -1 /
   'PROD100'  'PROD'  100 100  -1  'WATER'  -1 /
/
/

COMPDAT

  'INJ 1'  2*  1  988  'OPEN' -1 1 /
  'INJ 2'  2*  1  988  'OPEN' -1 1 /
  'INJ 3'  2*  1  988  'OPEN' -1 1 /
    .       .   .   .   .      .       .
    .       .   .   .   .      .       .
    .       .   .   .   .      .       .
    .       .   .   .   .      .       .
    .       .   .   .   .      .       .
    .       .   .   .   .      .       .
    .       .   .   .   .      .       .
    .       .   .   .   .      .       .
  'INJ 97'  2*  1  988  'OPEN' -1 1 /
  'INJ 98'  2*  1  988  'OPEN' -1 1 /
  'INJ 99'  2*  1  988  'OPEN' -1 1 /
  'INJ100'  2*  1  988  'OPEN' -1 1 /
   'PROD  1'  2*  1  988  'OPEN'  -1  1 /
   'PROD  2'  2*  1  988  'OPEN'  -1  1 /
   'PROD  3'  2*  1  988  'OPEN'  -1  1 /
    .       .   .   .   .      .       .
    .       .   .   .   .      .       .
    .       .   .   .   .      .       .
    .       .   .   .   .      .       .
    .       .   .   .   .      .       .
    .       .   .   .   .      .       .
    .       .   .   .   .      .       .
    .       .   .   .   .      .       .
   'PROD 97'  2*  1  988  'OPEN'  -1  1 /
   'PROD 98'  2*  1  988  'OPEN'  -1  1 /
   'PROD 99'  2*  1  988  'OPEN'  -1  1 /
   'PROD100'  2*  1  988  'OPEN'  -1  1 /
/

WCONINJE
 'INJ*'  'WATER' 'OPEN' 'RATE'   50  1.0E20  8.4 /
/

WCONPROD
 'PROD*'  'OPEN' 'LRAT' 1.0E20 1.0E20  1.0E20   50  1.0E20  1 /
/

WTRACER
```

```
   'INJ 1'  'DYE'  1  /
   'INJ 2'  'DYE'  1  /
   'INJ 3'  'DYE'  1  /
     .        .    .   .   .
     .        .    .   .   .
     .        .    .   .   .
     .        .    .   .   .
     .        .    .   .   .
     .        .    .   .   .
     .        .    .   .   .
     .        .    .   .   .
  'INJ 97'  'DYE'  1  /
  'INJ 98'  'DYE'  1  /
  'INJ 99'  'DYE'  1  /
  'INJ100'  'DYE'  1  /
/
```

C3 – Generic simulation DATA file for Z-permeability calculation.

```
-- RUNSPEC SECTION ================================================

RUNSPEC

TITLE
  Z-permeability Simulation

CART

-- Grid dimensions
DIMENS
-- Nx   Ny   Nz
 100   100   990 /

-- Dead oil Model used, phases are oil and water
WATER
OIL

-- Note LAB units are used throughout .DATA file
LAB

START
  01 'jan' 2011 /

WELLDIMS
-- NWMAX NWMAXZ NGMAX NWGMAX
  200    990     2    200 /

TABDIMS
-- NTSFUN   NTPVT    NSSFUN NPPVT
           1      1     100    100 /

TRACERS
   0    1    0    0 'NODIFF' /

-- Format output grid file

FMTOUT

NSTACK
-1 /

MESSAGES
  1000   1000   1000   1000   1000   1000   1000   1000   1000   1000   /

-- Unified format
UNIFOUT

-- GRID SECTION ===================================================

GRID

-- Use NEWTRAN for irregular grids and OLDTRAN for Cartesian grids
NEWTRAN
```

```
--Switch off output to the PRT file during grid loading to reduce output PRT file size
NOECHO

--Include file grid file
INCLUDE
 'Verticalpermgrid.grdecl' /

-- Give All Cells Same Porosity
PORO
9880000*0.3 /

--Include PERMX file for the specific case. Number at the end of filename indicates the % mud drape coverage for that case
INCLUDE
'TransmissibilityModel1Muddrapes20.grdecl' /

--make each grid block isotropic
COPY
'PERMX' 'PERMY' /
'PERMX' 'PERMZ' /
/

-- Buffer Layers with high Perm at the extreme ends of the grid are already defined in the grid file

-- Set up NNC's across pinched-out cells
PINCH
0.000001 'GAP' /

-- Produce initial file for GRAF
INIT

-- OUTPUT GRID
GRIDFILE
1 1 /

-- PROPERTIES SECTION  ============================================

PROPS

-- oil/water relative permeability and capillary pressure table (not used here since it is single phase)
--    Sw      Krw      Kro       Pcow
SWOF
          0         0                 1                 0
          0.485     0.000253906       0.1771875         0
          0.5186    0.00101752        0.112846278       0
          0.527     0.001365569       0.0999635         0
          0.5354    0.001802943       0.088216582       0
          0.5942    0.008970657       0.032282886       0
          0.6698    0.040664815       0.005171718       0
          0.7034    0.070376388       0.00156711        0
          0.7622    0.162248358       3.67416E-05       0
          0.8       0.26              0                 0
          1         1                 0                 0 /

-- Specify fluid properties
--        OIL      WATER      GAS
--      (g/cc)   (g/cc)   (g/cc)
DENSITY
        0.625     0.978      0.0/
```

```
-- Tracer names and their associated stock tank phases are defined using the tracer keyword

TRACER
 'DYE' 'WAT' /
/

-- Specify rock properties
--    REF.PRES   ROCK-COMPRESSIBILITY
--     (BAR)        (1/BAR)
ROCK
       2.00       0.000000145  /

-- Dead oil PVT table (FVF and Viscosity must vary with pressure)
--    Oil phase press.   Oil FVF   Oil Viscosity
--       (BAR)       ()    (CPoise)
PVDO
         0.4137      1.09    0.2900
         1.379      1.08    0.2901
         1.6547     1.07    0.2902
         1.9305     1.06    0.2903
         2.2063     1.05    0.2904
         2.4821     1.04    0.2905
         2.7579     1.03    0.2906
         3.0337     1.02    0.2907
         3.3095     1.01    0.2908
         4.5          1.009   0.2909
         6.11         1.008   0.2910
          8.4         1.007   0.2911       /

-- Water PVT table
--    Ref. press.  FVF-WATER  Compressibility  Viscosity  Viscosibility
--    (BAR)      ()     (1/BAR)     (CPoise)      (1/BAR)
PVTW
       2.00         1.0         0.00         0.31        0.0  /

--  REGIONS SECTION ====================================================

REGIONS

-- SOLUTION SECTION ====================================================

SOLUTION

EQUIL
-- for single phase water cases, equilibrate model by stting OWC at the tiop of or above the model dimensions
-- DATUM    PRESSURE    DEPTH    OWC    DEPTH    GOC    INIT   INIT   INTE
-- DEPTH    @ DATUM     OWC      CAP    GOC      CAP    TYPE   TYPE   N
--                        PRESS          PRE    LO     DO
  100       2.00       100      0.0   /

--Tracer concentrations
TVDPFDYE
100.0   0.0
100.0   0.0  /
/

-- SUMMARY SECTION ============================================================

SUMMARY
```

```
-- Specify creation of summary file
RPTSMRY
  1 /

RUNSUM

-- Specify output of oil and water in place to summary file
FOIP
FWIP
-- output liquid, oil,water production rate
FLPR
FOPR
FWPR
-- output field pressure
FPR
-- output water injection rate
FWIR
-- output well pressures
WBP5
FTPRDYE
FTPTDYE
/

-- SCHEDULE SECTION ============================================================

SCHEDULE

RPTRST
POT /

-- Include file containing WELSPECS, WCONPROD and WCONINJE keywords
INCLUDE
   'welspecsa.ecl' /

WPAVE
1.0 0.5 /

-- Specify performance of solver (requirements vary for each case)

TUNING
0.1 1.5               /
                      /
2* 200 1* 4           /

NUPCOL
15 /

ECHO

--time to reach steady state id short. Simualtions for as low as 2 hrs were used. Some were simulated longer
TSTEP
10*0.2 /

RPTSCHED
'RESTART = 1' 'FIPTR=2' /

END
```

Welspecs file for Z perm

```
--
WELSPECS
 'INJ 50'   'INJ'  50    50   -1  'WATER' -1 /
 'PROD 50'  'PROD' 50    50  -1  'WATER' -1 /
/

COMPDAT
 'INJ 50'   2*   1     1   'OPEN' -1 1 /
 'PROD 50'  2*   990   990 'OPEN' -1 1 /
/

WCONINJE
 'INJ 50'  'WATER' 'OPEN' 'RATE'   1  1.0E20  8.4 /
/

WCONPROD
 'PROD 50'  'OPEN' 'LRAT' 1.0E20 1.0E20  1.0E20   1  1.0E20  1 /
/

WTRACER
'INJ  50' 'DYE'    1          /
```